

THERMAL POSTBUCKLING / TRANSVERSE DEFLECTIONS OF
ANGLE- AND CROSS-PLY LAMINATED PLATES

*A Thesis submitted
In Partial Fulfillment of the requirements
for the Degree of*
MASTER OF TECHNOLOGY

by

NAVNEET KISHORE DIXIT

to the

DEPARTMENT OF CIVIL ENGINEERING
INDIAN INSTITUTE OF TECHNOLOGY, KANPUR
JUNE 1993

DEDICATED
TO
TO MY PARENTS AND BROTHER

CE-1993-M-DIX-THE

2 DEC 1993/CE
CENTRAL LIBRARY
F I T S A D I R

Acc. No. A 114757

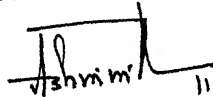
TH
E 24.184
A 642 t

11.6.93
Bo

CERTIFICATE

This is to certify that the research carried out by NAVNEET KISHORE DIXIT for the preparation of the thesis, 'THERMAL POSTBUCKLING / TRANSVERSE DEFLECTIONS OF ANGLE- CROSS-PLY LAMINATED PLATES' , has been supervised by me. This thesis is being submitted to the Department of Civil Engineering, Indian Institute of Technology, Kanpur, in partial fulfillment of the requirements for the degree of MASTER OF TECHNOLOGY, and has not been submitted for a degree elsewhere.

June, 1993


11.6.93
ASHWINI KUMAR

PROFESSOR

Department of Civil Engineering

Indian Institute of Technology

Kanpur - 208016

INDIA

ACKNOWLEDGEMENTS

I express my deep sense of gratitude to Dr. Ashwini Kumar for his invaluable suggestions and untiring guidance. I would be failing in my duty if I do not express my grateful thanks to Dr. N. G. R. Iyengar for introducing me to the subject of composite structures.

I sincerely thank my friend Murali Mohan for his useful suggestions and discussion. I am also grateful to Arvind Galgali who helped me in his own way.

Thanks are also due to all my friends who made my stay at I.I.T. Kanpur a pleasant one.

Finally, the financial support received through a research grant from the A.R.D.B. is gratefully acknowledged.

NAVNEET K. DIXIT

CONTENTS

TITLE	Page No.
CERTIFICATE	(i)
ACKNOWLEDGEMENTS	(ii)
LIST OF FIGURES	(iv)
NOTATIONS	(vi)
ABSTRACT	
1 INTRODUCTION	1
1.1 Introductory Remark	1
1.2 Literature Review	3
1.3 Aim of Investigation	7
1.4 Statement of the Problem	7
2 FORMULATION AND SOLUTION TECHNIQUE	11
2.1 Introduction	11
2.2 Displacements and Strains	13
2.3 Total Potential Energy	14
2.4 Application of Rayleigh Ritz Method	16
3 NUMERICAL RESULTS AND DISCUSSION	19
3.1 Introduction	19
3.2 Uniform Temperature Response	21
Antisymmetric Angle-ply Laminates	21
Symmetric Cross-ply Laminates	26
Antisymmetric Cross-ply Laminates	27
Angle-ply Vs. Cross-ply	30
3.2 Non-Uniform Temperature Response	31
4 CONCLUSIONS	50
4.1 Concluding Remarks	50
4.2 Recommendations for Future Work	51
REFERENCES	52
APPENDIX 1	54
1.1 Stress-Strain Relations for a Lamina	54
1.2 Strain variation in a Lamina	57
1.3 Resultant Laminate Forces and Moments	58
APPENDIX 2	60
2.1 Antisymmetric Angle-ply	60
2.2 Symmetric Angle-ply	60
2.3 Symmetric Cross-ply	61
2.4 Antisymmetric Cross-ply	61

LIST OF FIGURES

No.	Title	Page No.
1.1-1.2	Geometric boundary conditions considered in the present analysis	10
3.1-3.6	Center deflection of antisymmetric angle-ply ($\theta=45^\circ$) subjected to uniform temperature Boundary conditions : Type 1	33
3.7-3.12	Center deflection of antisymmetric angle-ply ($\theta=22.5^\circ$) subjected to uniform temperature Boundary conditions : Type 1	35
3.13-3.21	Center deflection of antisymmetric angle-ply subjected to uniform temperature Boundary conditions : Type 1	37
3.22-3.25	Center deflection of antisymmetric angle-ply ($\theta=45^\circ$) subjected to uniform temperature Boundary conditions : Type 2	40
3.26-3.29	Center deflection of antisymmetric angle-ply ($\theta=45^\circ$) subjected to uniform temperature Boundary conditions	41
3.30-3.32	Center deflection of symmetric cross-ply subjected to uniform temperature Boundary conditions : Type 1	42
3.33-3.36	Center deflection of antisymmetric cross-ply subjected to uniform temperature	43

	Boundary conditions : Type 1	
3.37-3.40	Center deflection of antisymmetric cross-ply subjected to uniform temperature	44
	Boundary conditions : Type 2	
3.41-3.42	Center deflection of antisymmetric cross-ply subjected to uniform temperature	45
3.43-3.45	Center deflection of antisymmetric angle-ply ($\theta=45^\circ$) Boundary conditions : Type 1	46
3.46-3.48	Center deflection of antisymmetric angle-ply ($\theta=22.5^\circ$) Boundary conditions : Type 1	47
3.49-3.51	Center deflection of antisymmetric angle-ply ($\theta=45^\circ$) Boundary conditions : Type 2	48
3.52-3.53	3-D plot showing mode shape of 22.5° angle- ply laminate	49
A1.1	Orthotropic lamina along the principal axes	55
A1.2	Orthotropic lamina oriented at an angle θ with structural axes	56
A1.3	Geometry of an N-layered laminate	59

NOTATIONS

a, b	Dimensions of the plate in the X-direction and Y-directions respectively
$[A], [B], [C]$	Extensional, coupling and bending stiffness matrix respectively
c	Coefficient, which controls the magnitude of temperature gradient through-the-thickness of the plate
E_L	Longitudinal elastic modulus for a composite lamina
E_T	Transverse elastic modulus for a composite lamina
f_1 to f_9	Linear functions in Eq.(3.9)
G_{LT}	Shear modulus in the L-T plane
g_1 to g_5	Nonlinear functions in Eq.(3.9)
H	Thickness of the plate in Z-direction
M_x, M_y, M_{xy}	Resultant moments acting on a laminates per unit length of the edge
M_x^T, M_y^T, M_{xy}^T	Thermal moments
N_x, N_y, N_{xy}	Resultant in-plane forces on a laminate (per unit length)
N_x^T, N_y^T, N_{xy}^T	Thermal forces
N	Number of layers in a laminate
Q_{ij}	Reduced stiffnesses of an orthotropic lamina

\bar{Q}_{ij}	Transformed reduced stiffnesses of an orthotropic lamina
T	Temperature change at the midplane of the plate
T	Normalizing buckling temperature
ΔT	Temperature change at any point of the plate
u_0, v_0	Midplane values of inplane displacements
u, v	Inplane displacement at any point of laminate
u_{ij}, v_{ij}	Approximating inplane shape function
u,x, v,x, u,y, v,y	Derivative of inplane displacement with respect to the suffix that follows
U	Strain energy of rectangular plate
V	Total potential energy of the plate
V_T	Potential energy due to the thermal forces and moments
V	Volume of the plate
w	Transverse displacement of the plate
w_{mn}	Approximating out-of-plane shape function
$w,x, w,y, w,xx, w,xy, w,yy$	Derivative of lateral displacement with respect to the suffix that follows
w_0	Central out-of-plane displacement of plate
z_k, z_{k-1}	Defined in Fig. A1.3
α_L, α_T	Coefficient of thermal expansion in L- and T-directions respectively
α_x, α_y	Coefficient of thermal expansion in X- and Y-directions respectively

α_{xy}	Apparent coefficient of thermal shear
θ	Lamination angle
$\epsilon_x, \epsilon_y, \gamma_{xy}$	Strain components in L-T plane
$\epsilon_x, \epsilon_y, \epsilon_{yy}$	Strain components in X-Y plane
$\{\epsilon_L^o\}$	Midplane strain vector with linear terms
$\{\epsilon_{NL}^o\}$	Midplane strain vector with nonlinear terms
$\sigma_L, \sigma_T, \tau_{LT}$	Stress components in L-T plane
$\sigma_x, \sigma_y, \tau_{xy}$	Stress components in X-Y plane
K_x, K_y, K_{xy}	Middle surface curvature
ν_{LT}	Poisson's ratio

ABSTRACT

The present investigation deals with the postbuckling response of the simply supported angle- and cross-ply laminated plates under thermal loads. The Rayleigh Ritz energy technique is used to obtain the governing nonlinear algebraic equations by assuming a double series form of trial functions for the displacement fields. A computer program is developed to solve nonlinear algebraic equations. The effect of boundary conditions, the fiber orientation, the number of lay-ups and the aspect ratio on the transverse deflection is studied. The analysis is carried out for uniform temperature throughout the plate as well as for slight temperature gradient through-the-thickness of the plate. Results are presented in the graphical form for antisymmetric angle-ply and symmetric and antisymmetric cross-ply laminates.

CHAPTER 1

INTRODUCTION

1.1 INTRODUCTORY REMARKS :

It is well known that the measured strengths of most of the materials are found to be much smaller than their theoretical strengths. The discrepancy in strength values is believed to be due to the presence of imperfections or inherent flaws in the material. The flaws in the form of cracks that lie perpendicular to the direction of applied loads are particularly detrimental to the strength. Therefore, compared with the strength of bulk material, man-made filaments or fibers exhibit much higher strength along their lengths since large flaws, which may be present in the bulk material, are minimized because of small cross-sectional area of the fibers. Fibers, because of their small cross-sectional dimensions, are not directly usable in the engineering applications. They are, therefore, embedded in the matrix materials to form fibrous composites. The matrix serves to bind the fibers together, transfer loads to the fibers and protect them against environmental attacks and damages due to handling.

Laminated composite plates are made of plies, each ply being composed of straight, parallel fibers (e.g., glass, boron, graphite) embedded in and bonded together by a matrix material

(e.g epoxy resin) Each ply may be considered as homogeneous, orthotropic material having a value of Young's modulus(E) considerably greater in the longitudinal direction than in the transverse direction. Adjacent plies will have longitudinal axes usually not parallel. Cross-ply laminated plates arise in the special case when the longitudinal axes of the adjacent plies are perpendicular, whereas angle-ply laminates occur when adjacent layers are alternatively oriented at angles of $+\theta$ and $-\theta$ with respect to the edges of the plate.

Fiber-reinforced composite laminates have high strength-to-weight and stiffness-to-weight ratios and are becoming important in weight-sensitive applications such as spacecraft and space vehicles. A re-entry space vehicle encounters hyperthermal loading conditions. In certain cases, the thermal load turns out to be the primary one and controls the design. The availability of composites and use of optimization techniques in the design for minimum weight results in structures which are very thin. The plate elements, which are extensively used in aircraft construction, are subjected to compressive stresses due to boundary constraints. Therefore, the thermal loads may cause buckling, especially in thin-walled structures. Though the investigation of thermally-induced buckling of composite plate is in itself an important aspect, the study of the postbuckling response, specially in the presence of a temperature gradient through-the-thickness of plate, assumes a far greater importance.

As with the mechanical loading, composite plate should be expected to operate in the postbuckling range with thermal loads as well, if structural efficiencies are to be high. Restricting the temperature to remain below the buckling temperature, or designing stiffnesses so that plates do not buckle, are inefficient approaches to thermal structural design. Moreover, buckling is actually an idealization of the problem. Generally, the geometric imperfections in the plate, the support conditions and even imperfections in the assumed temperature field preclude the occurrence of the ideal buckling (bifurcation), thus necessitating the study of the postbuckling response of such plates. This forms the scope of the present investigation.

1.2 LITERATURE REVIEW :

A recent review article by Tauchert (1991) on thermally-induced flexure, buckling and vibration of plates gives an up-to-date account of buckling of composite plates, under thermal loads. Postbuckling of plates is an important topic and has attracted the attention of many researches over the past several decades. A detailed literature review on thermal postbuckling of isotropic and orthotropic plates has been covered in the article by Tauchert (1991).

Most of the early investigations on the subject of thermal postbuckling have been devoted to isotropic thin plates and shells. Based on the large deflection theory, Gossard (1952) used

the Rayleigh-Ritz method to calculate the deflections of flat or initially imperfect plates subjected to nonuniform temperature distributions. The postbuckling behaviour of rectangular plates which are heated symmetrically about the two center lines was investigated by Forray and Newman (1962a). Soon afterwards they solved the same problem by the combined Rayleigh-Ritz and Galerkin procedure which permits more flexibility in the choice of boundary conditions (1962b). A method for the analysis of a rectangular plate heated nonuniformly and allowed to undergo large deflections was presented by Wilcox and Clemmer (1964). Mahayani (1966) studied the thermal buckling and postbuckling response of a simply supported cylindrical panels subjected to parabolic temperature distribution along its radial direction. Thermal postbuckling characteristics of skew plates with restrained edges were analyzed by Prabhu and Druvasula (1976). Following Berger's method, the large deflection of a heated cylindrical shell was investigated by Biswas (1978a). He also presented an analysis for the large deflections of a heated orthotropic plate (1978b). Banerjee and Datta (1979) studied the large deflections of simply supported isotropic plates of any given shape under a varying temperature distribution. Biswas (1981) obtained an approximate solution of the governing equations for a heated orthotropic plate. A simple thermal postbuckling analysis of isotropic circular plates was carried out by Raju and Rao (1984).

Compared to isotropic cases, relatively few investigations

have been made on the thermal postbuckling behaviour of laminated composite plates. Thermal buckling and postbuckling behaviour of antisymmetric angle-ply plates, resting on simple supports and subjected to uniform temperature rise, was examined by Tauchert and Huang (1986). Since the closed-form solutions to the resulting coupled nonlinear equations are not easy, a direct application of the principle of minimum potential energy had been applied to obtain approximate solutions. Numerical results for graphite/epoxy laminates illustrated the effects of number of lay-ups, the ply angle and the aspect ratio of the plate upon thermoelastic response. Huang and Tauchert (1988a) again analyzed the same problem, but here the emphasis was given to secondary buckling. The effect of fiber orientation, number of lay-ups and the aspect ratio was also carried out. The scope of this study was enlarged in a subsequent investigation (Huang and Tauchert, 1988b) in which the nonuniform temperature field was considered. They showed that unlike the uniform temperature problem in which the simply supported laminate remains flat until bifurcation occurs, under a nonhomogeneous temperature field, the transverse deflections occur immediately upon loading. In such cases a bifurcation may occur, however, at a later stage of thermal loading. A major effort in dealing with the problem of thermally-induced large deflections by finite element method was made by Chen and Chen (1989). They carried out the study of geometrically nonlinear response of composite plates under a nonuniform temperature field. The analysis showed that the

postbuckling behaviour is influenced by the lamination angle, the plate aspect ratio, the modulus ratio and the number of layers. The large-deflection response of laminates under thermal loading, including flat plates and cylindrical panels, was investigated by Huang and Tauchert (1990). The finite element formulation based on the first order shear deformation theory was employed to predict the shell response. The strength limit of laminates had been predicted using Tsai-Wu criterion. With change in temperature, thermal and elastic properties (e.g. coefficient of thermal expansion, E_L , E_T , etc) do not remain constant. Chen and Chen (1991) examined the effect of temperature dependent properties on thermal postbuckling behaviour of laminated plates. It was found that the postbuckling strength reduced significantly when temperature-dependent properties were taken into consideration. Meyer and Heyer (1992) analyzed the thermally-induced geometrically nonlinear response of symmetrically laminated plates. The plate response was considered due to a temperature increase that was uniform in the plane of plate but had a slight temperature gradient through-the-thickness of plate. The case of a completely uniform temperature increase but with initial out-of-plane imperfection was also considered. The study showed that difference between buckling temperatures for the fixed and the sliding simple supports is small and that the support conditions can have large influence on the thermally-induced nonlinear response. It was also shown that the geometric as well as temperature imperfections play an important

role in the initial out-of-plane deflections

1.3 AIM OF INVESTIGATION .

The forgoing literature review clearly shows that only a few research works have been carried out on laminated composite plates subjected to temperature loading. It is also clear that no results are available for thermally induced large deflections of cross-ply laminated plates. The aim of the present work is to study the postbuckling response of antisymmetric angle-ply and cross-ply laminated plates, under two types of temperature fields : (i) uniform temperature increase throughout the plate, (ii) temperature increase that is uniform in the plane of plate but has a slight gradient through-the-thickness.

The effect of the number of lay-ups, the fiber orientation and the aspect ratio of the plate on thermally-induced nonlinear response is considered.

1 4 STATEMENT OF THE PROBLEM .

A plate as shown in the Fig. 1.1-1 2, with length a , width b and thickness H is considered. The reference co-ordinate system has its origin at one corner of the plate. The x - y plane coincides with the geometric midplane of the plate, and z -axis points downwards. The geometric midplane is the reference surface

of the plate. The temperature change, ΔT , is given by

$$\Delta T = T(1.0 + c.z/H) \quad (1.1)$$

where T is the temperature change at the midplane of the plate. The parameter c controls the magnitude of the through-the-thickness gradient. Referring to the co-ordinate system mentioned, the temperature change at the top of plate is $T(1.0 - c/2.0)$, and that at the bottom is $T(1.0 + c/2.0)$. This can as well represent an imperfection in the temperature distribution which will cause the plate to begin to deflect out of plane as soon as the temperature increases relative to the reference temperature.

The problem can be also analyzed for following cases :

- (i) $c = 0$, i.e , the plate is subjected to uniform temperature
- (ii) Linearly varying transverse temperature distribution given by $\Delta T = (T.c).z/H$ where, now, $T.c$ denotes the temperature difference across the plate thickness. Cases (i) and (ii) can in fact be superimposed to get a distribution of the type given by Eq. (1.1). Both the angle-ply and the cross-ply laminated plates are included in the study. Two boundary conditions have been considered :
- (i) fixed simple support conditions : all four edges are fixed against in-plane normal and tangential displacements as well as out-of-plane displacements (Fig.1.1), (ii) sliding simple supports : all four edges are fixed against in-plane normal and out-of-plane displacements, but are free to move or slide tangentially(Fig.1.2). Sliding is assumed frictionless. These

boundary conditions can be expressed as :

Fixed simple supports (referred to as type 1)

Along $x = 0, a$

$$u_0 = 0, v_0 = 0, w = 0, M_x = 0$$

Along $y = 0, b$

$$u_0 = 0, v_0 = 0, w = 0, M_y = 0 \quad (1.2)$$

Sliding simple supports (referred to as type 2)

Along $x = 0, a$

$$u_0 = 0, N_{xy} = 0, w = 0, M_x = 0$$

Along $y = 0, b$

$$N_{xy} = 0, v_0 = 0, w = 0, M_y = 0 \quad (1.3)$$

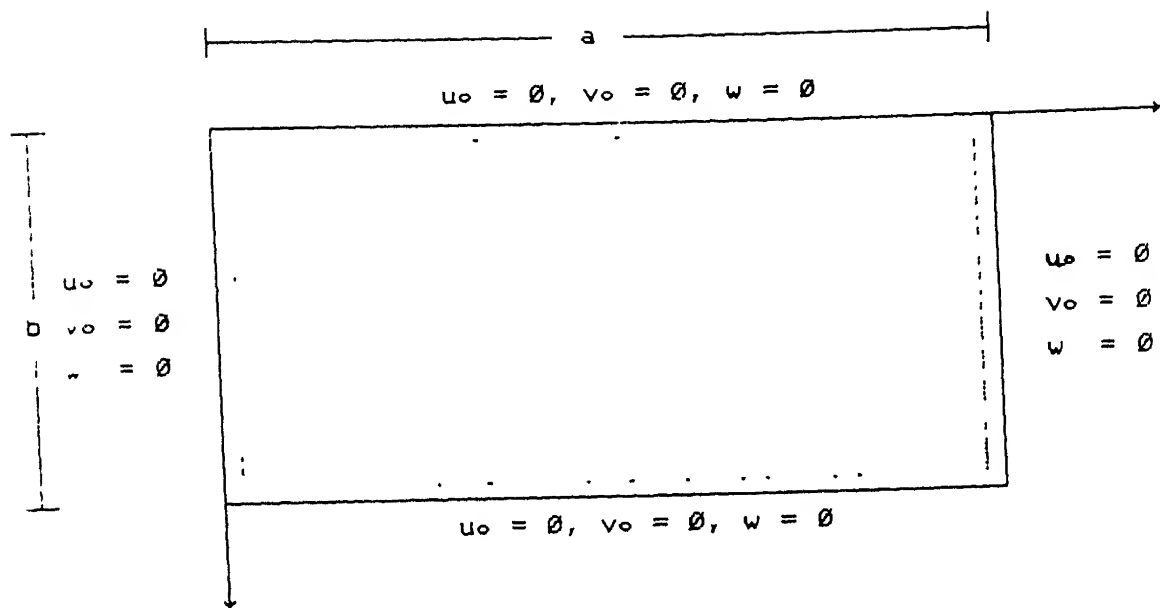


Fig. 1.1 Boundary conditions : Fixed simple supports

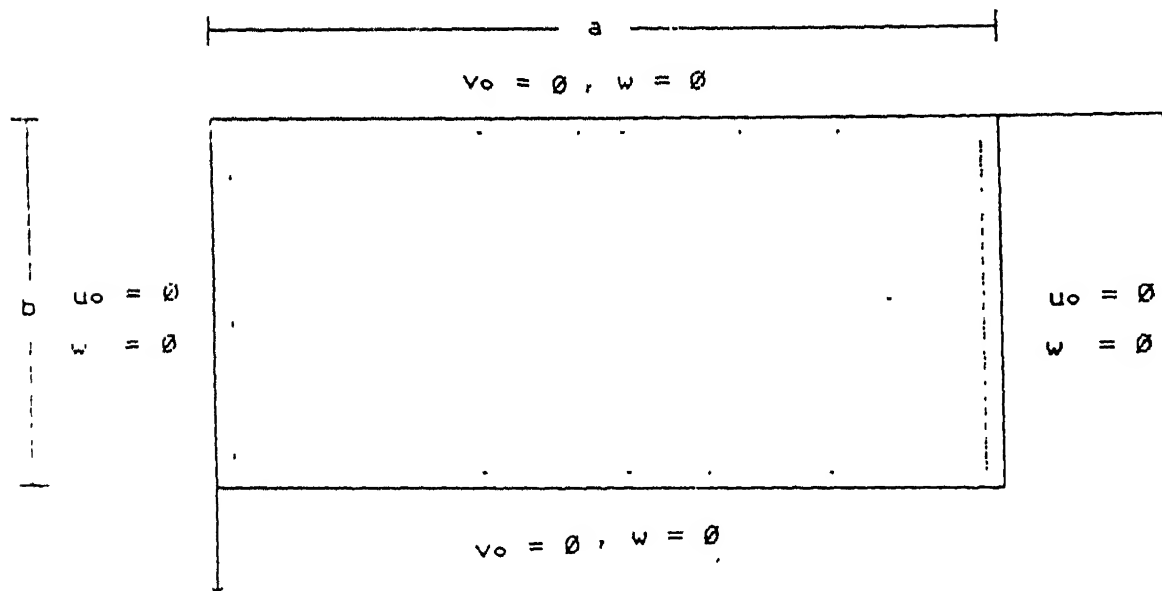


Fig. 1.2 Boundary conditions : Sliding simple supports

CHAPTER 2

FORMULATION AND SOLUTION TECHNIQUE

2.1 INTRODUCTION :

In most practical applications, the thickness of a plate is small in comparison with its smallest lateral dimension, and hence Kirchhoff's hypothesis may be assumed to be valid. This implies that tractions on the surfaces parallel to reference plane are negligibly small as compared with the inplane stresses, and that the inplane displacements are linear functions of z .

The determination of the buckling temperature load for a particular structure, say a thin plate, is essentially an eigen-value problem based on linear (small deflection theory) but this type of analysis yields only the buckling temperature and does not give any information about the magnitude of the lateral deflection at the onset of buckling (of plate) and beyond. Therefore, the use of non-linear equation, based on the large deflection theory, becomes essential for studying the behaviour of thin plate in the postbuckling regime. The von karman equations are most widely used equations for this purpose. Although these equations are available in various forms their analytical solution is not possible in most of the cases. Out of the many numerical methods available to solve these nonlinear equations the Rayleigh

Ritz method turns out to be quite convenient for a wide class of problems.

The Rayleigh Ritz technique or simply the Ritz technique is a procedure for applying the principle of minimum potential energy to obtain approximate solutions of elastic problems. In case of plate problems where the three displacement components u , v and w are to be determined, the procedure consists essentially in assuming that the desired extremal of a given problem can be approximated by linear combinations of suitably chosen functions in the following form

$$\begin{aligned} u &= \sum_{i=1}^I \sum_{j=1}^J A_{ij} u_{ij}(x,y) \\ v &= \sum_{i=1}^I \sum_{j=1}^J B_{ij} v_{ij}(x,y) \\ w &= \sum_{m=1}^M \sum_{n=1}^N C_{mn} w_{mn}(x,y) \end{aligned} \quad (2.1)$$

In these expressions A_{ij} , B_{ij} and C_{mn} are the undetermined parameters and u_{ij} , v_{ij} and w_{mn} are the known functions, each of which can be written as $F_i(x) G_j(y)$. These functions are chosen such that they are continuous, satisfy at least the prescribed geometric or kinematic boundary conditions for any choice of these parameters, and are capable of representing the deformed shape of the plate problem. When Eq.(2.1) is substituted into the potential energy expression, the latter becomes the function of parameters A_{ij} , B_{ij} and C_{mn} . These parameters are determined from

the condition that the total potential energy of the system is minimum with respect to them. This condition gives the same number of equations for A_{ij} , B_{ij} and C_{mn} as the number of parameters taken. The accuracy of the method depends upon the choice of the number of parameters and the approximating shape functions u_{ij} , v_{ij} and w_{mn}

2.2 DISPLACEMENTS AND STRAINS :

In view of the Kirchhoff's assumption of thin plate theory, the inplane displacements u , v and w at any arbitrary point of the plate in the x -, y - and z -directions can be approximated by

$$\begin{aligned} u(x,y,z) &= u_0(x,y) - z.w,x \\ v(x,y,z) &= v_0(x,y) - z.w,y \\ w(x,y,z) &= w(x,y) \end{aligned} \quad (2.2)$$

where u_0 , v_0 are the mid-surface inplane displacements and a comma signifies the derivative with respect to suffix that follows.

In view of the von Karman theory of large deflection of plates, the strain displacement relationship can be written as

$$\begin{aligned} \epsilon_x &= \partial u_0 / \partial x + (1/2)(\partial w / \partial x)^2 - z (\partial^2 w / \partial x^2) \\ \epsilon_y &= \partial v_0 / \partial y + (1/2)(\partial w / \partial y)^2 - z (\partial^2 w / \partial y^2) \\ \gamma_{xy} &= \partial v_0 / \partial x + \partial u_0 / \partial y + (\partial w / \partial x)(\partial w / \partial y) - 2 z (\partial^2 w / \partial x \partial y) \end{aligned} \quad (2.3)$$

In short, these can be written as

$$[\epsilon] = [\epsilon_L^0] + [\epsilon_{NL}^0] + z [K] \quad (2.4)$$

where $[\epsilon^0]$ are the mid-plane strains, which include terms which account for stretching due to transverse displacement w . These terms are seen to be nonlinear $[K]$ are the curvature changes of the mid-plane during deformations. These are functions of x and y only.

2.3 TOTAL POTENTIAL ENERGY :

The total potential energy V of a structure is the sum of the strain energy U stored in the rectangular plate and the potential energy V_T due to the thermal forces and moments, i.e.

$$V = U + V_T \quad (2.5)$$

The strain energy U stored in a rectangular laminated plate, which is assumed to be in a state of plane stress, can be expressed as

$$U = \frac{1}{2} \int_V [\sigma] \{\epsilon\} dv \quad (2.6)$$

$$U = \frac{1}{2} \int_V [\epsilon] [\bar{Q}] \{\epsilon\} dv$$

Using the Eqs. (A1.3), (A1.6) and (A1.10) from Appendix 1 and the subsequent integration with respect to z yields

$$\begin{aligned}
U = \int_0^b \int_0^a [& A_{11} (u,x + 1/2 w_{,x}^2)^2 + 2 A_{12} (v,y + 1/2 w_{,y}^2) * \\
& (u,x + 1/2 w_{,x}^2) + 2 A_{16} (u,y + v,x + w,x w,y) (u,x + 1/2 w_{,x}^2) + \\
& 2 A_{26} (u,y + v,x + w,x w,y) (v,y + 1/2 w_{,y}^2) + A_{22} (v,y + 1/2 w_{,y}^2)^2 \\
& + A_{66} (u,y + v,x + w,x w,y)^2 - 2 \{ B_{11} (u,x + 1/2 w_{,x}^2) w_{,xx} + \\
& B_{12} (v,y + 1/2 w_{,y}^2) w_{,xx} + B_{16} (u,y + v,x + w,x w,y) w_{,xx} + \\
& B_{12} (u,x + 1/2 w_{,x}^2) w_{,yy} + B_{22} (v,y + 1/2 w_{,y}^2) w_{,yy} + \\
& B_{26} (u,y + v,x + w,x w,y) w_{,yy} + 2 B_{16} (u,x + 1/2 w_{,x}^2) w_{,xy} + \\
& 2 B_{26} (v,y + 1/2 w_{,y}^2) w_{,xy} + \\
& 2 B_{66} (u,y + v,x + w,x w,y) w_{,xy} \} + D_{11} w_{,xx}^2 + 2 D_{12} w_{,yy} w_{,xx} + \\
& 4 D_{16} w_{,xy} w_{,xx} + D_{22} w_{,yy}^2 + 4 D_{26} w_{,xy} w_{,yy} + D_{66} w_{,xy}^2] dx dy
\end{aligned}
\tag{2.7}$$

In the preceding expression the subscript o of u_o and v_o have been dropped for convenience.

The potential energy due to thermal forces and moments can be written as

$$\begin{aligned}
V_T = \int_0^b \int_0^a [& -N_x^T (u,x + 1/2 w_{,x}^2) - N_y^T (v,y + 1/2 w_{,y}^2) - \\
& N_{xy}^T (u,y + v,x + w,x w,y) + M_x^T w_{,xx} + M_y^T w_{,yy} + 2 M_{xy}^T w_{,xy}] dx dy
\end{aligned}
\tag{2.8}$$

The relevant expressions for thermal forces and moments are presented in the Appendix 1 (see A.14).

2.4 APPLICATION OF RAYLEIGH RITZ METHOD

The geometric boundary conditions of the present problem can be satisfied by assuming a double series form of a trial function for the displacements. They are given below for the two types of edge conditions considered (section 1.4).

Type 1 (i.e. fixed simple support)

$$\begin{aligned}
 u_0(x,y) &= \sum_{i=1}^I \sum_{j=1}^J u_{ij} \sin(i\pi x/a) \sin(j\pi y/b) \\
 v_0(x,y) &= \sum_{i=1}^I \sum_{j=1}^J v_{ij} \sin(i\pi x/a) \sin(j\pi y/b) \\
 w(x,y) &= \sum_{m=1}^M \sum_{n=1}^N w_{mn} \sin(m\pi x/a) \sin(n\pi y/b)
 \end{aligned} \tag{2.9}$$

Type 2 (i.e. sliding simple support)

$$\begin{aligned}
 u_0(x,y) &= \sum_{i=1}^I \sum_{j=0}^J u_{ij} \sin(i\pi x/a) \cos(j\pi y/b) \\
 v_0(x,y) &= \sum_{i=0}^I \sum_{j=1}^J v_{ij} \cos(i\pi x/a) \sin(j\pi y/b) \\
 w(x,y) &= \sum_{m=1}^M \sum_{n=1}^N w_{mn} \sin(m\pi x/a) \sin(n\pi y/b)
 \end{aligned} \tag{2.10}$$

These series are substituted in the total potential energy V

obtained by using Eqs (2.7) and (2.8) in Eq (2.5). Then the Ritz equations are obtained by setting

$$\begin{aligned}\partial V / \partial u_{ij} &= 0 \\ \partial V / \partial v_{ij} &= 0 \\ \partial V / \partial w_{mn} &= 0\end{aligned}\quad (2.11)$$

This results in a coupled set of nonlinear algebraic equations.

Which can be written in following general form :

$$\sum_p \sum_q \sum_i \sum_j u_{ij} f_1 + \sum_p \sum_q \sum_i \sum_j v_{ij} f_2 + \sum_p \sum_q \sum_m \sum_n w_{mn} f_3 = -g_1 + N_1$$

$$\sum_p \sum_q \sum_i \sum_j u_{ij} f_4 + \sum_p \sum_q \sum_i \sum_j v_{ij} f_5 + \sum_p \sum_q \sum_m \sum_n w_{mn} f_6 = -g_2 + N_2$$

$$\begin{aligned}\sum_p \sum_q \sum_i \sum_j u_{ij} (f_7 + g_3) + \sum_p \sum_q \sum_i \sum_j v_{ij} (f_8 + g_4) + \sum_p \sum_q \sum_m \sum_n w_{mn} f_9 = -g_5 \\ + N_3\end{aligned}\quad (2.12)$$

where N_1 , N_2 and N_3 are

$$N1 = \int_0^a \int_0^b [N_x^T(p\pi/a) \cos(p\pi x/a) \sin(q\pi y/b) + N_{xy}^T(q\pi/a) \sin(p\pi x/a) \cos(q\pi y/b)] dx dy$$

$$N2 = \int_0^a \int_0^b [N_y^T(q\pi/b) \sin(p\pi x/a) \cos(q\pi y/b) + N_{xy}^T(p\pi/a) \cos(p\pi x/a) \sin(q\pi y/b)] dx dy$$

$$N3 = \int_0^a \int_0^b [M_x^T(p\pi/a)^2 \sin(p\pi x/a) \sin(q\pi y/b) + M_y^T(q\pi/b)^2 \sin(p\pi x/a) \sin(q\pi y/b) - 2M_{xy}^T(p\pi/a) (q\pi/b) \cos(p\pi x/a) \cos(q\pi y/b)] dx dy$$

In Eq. (2.12) f_1 to f_9 are linear expressions, while g_1 to g_5 are nonlinear expressions. Where g_5 contains cubic as well as square terms. To solve these coupled set of nonlinear algebraic equations, a computer program has been developed. This program uses standard subroutines available in the NAG library for single integration, double integration and for the solution of nonlinear equations. The solution of various cases are presented and discussed in the next chapter.

CHAPTER 3

NUMERICAL RESULTS AND DISCUSSION

3.1 INTRODUCTION :

The formulation developed in the chapter 2 has been first checked by comparing the results with some of those available in the literature for antisymmetric angle-ply laminates and symmetric laminates. It is then employed to estimate the transverse deflection of antisymmetric angle-ply and symmetric and antisymmetric cross-ply laminates, each consisting of N equal-thickness layers. The a/H ratio (plate length to thickness ratio) considered is 150. The material properties used in the analysis represent a graphite-reinforced composite. These properties are :

$$\begin{aligned} E_L &= 155 \text{ GPa} & E_T &= 8.07 \text{ GPa} & G_{LT} &= 4.55 \text{ GPa} & \nu_{LT} &= 0.22 \\ \alpha_L &= -0.07 \times 10^{-6} \text{ }^\circ\text{C}^{-1} & \alpha_T &= 30.1 \times 10^{-6} \text{ }^\circ\text{C}^{-1} \end{aligned}$$

The above parameters are defined in the principal material system of a layer and follow the usual notation. For the case of temperature gradient through-the-thickness of the plate, results are presented for $c = 0.05$ in Eq.(1.1). This value of c means that the plate is 5 % warmer on the bottom than on the top.

A continuously varying change in temperature from an ambient

temperature is represented by a sequence of incremental temperature changes. At each increment a new solution must be found. The search for a new solution, at each temperature increment, is begun by taking as an initial guess the solution obtained for the preceding temperature step. A total of nine terms are taken in the series for u_0 and v_0 in Eqs. (2.9) and (2.10) to approximate the inplane displacements. Typically, a total of four terms are taken in the series for w to approximate the transverse deflection. The selection of most significant terms for a particular laminate and the loading is generally a matter of trial and error. Various combinations of terms are tried until the predominant modes for a particular case under consideration are identified. Transverse deflection W_0 at the center of plate (normalized with respect to laminate thickness H) is plotted as a function of T , the change in temperature at the midplane of the laminate (normalized with respect to T^*). For plates subjected to uniform temperature, T represents the temperature change at every point in the plate, not just at the the midplane. The buckling temperature (30.6°C) of the four-layer square antisymmetric angle-ply ($\theta=45^\circ$) plate with fixed simple supports has been taken as the reference value T^* for antisymmetric angle-ply laminates, while for cross-ply laminates T^* is the buckling temperature (28.6°C) of a square symmetric cross-ply laminate with fixed simple supports. These values are very close to those for an orthotropic plate (i.e.

for large number of layers) and hence are taken as the reference values

Results are presented for the following two cases :

- (i) Plate subjected to uniform temperature (Figs. 3.1 to 3.42)
- (ii) Plate subjected to non-uniform temperature field (Figs. 3.43 to 3.51)

3.2 UNIFORM TEMPERATURE RESPONSE

Antisymmetric angle-ply laminates

Consider the postbuckling response of an antisymmetric angle-ply laminate subjected to a uniform increasing temperature field T . Using Eq. (A1.14) of Appendix 1, it can be shown that for this case the thermal force N_{xy}^T and the thermal moments M_x^T , M_y^T are zero. For this type of laminates, the boundary conditions become

Fixed simple supports (type 1) :

along $x = 0, a$

$u_0 = 0, v_0 = 0, w = 0$ and

$$M_x = B_{16}(u,y + v,x + w,x w,y) - D_{11}w,xx - D_{12}w,yy = 0$$

along $y = 0, b$

$u_0 = 0, v_0 = 0, w = 0$ and

$$M_y = B_{26}(u,y + v,x + w,x w,y) - D_{12}w,xx - D_{22}w,yy = 0$$

(3.1)

Sliding simple support (type 2) :

CENTRAL LIBRARY
I. I. T., KANPUR

Acc. No. A. 116757

along $x = 0, a$

$$w = 0, \quad M_x = B_{16}(u,y + v,x + w,x w,y) - D_{11}w,xx - D_{12}w,yy = 0$$

$$u_0 = 0, \quad N_{xy} = A_{66}(u,y + v,x + w,x w,y) - B_{16}w,xx - B_{26}w,yy = 0$$

along $y = 0, b$

$$w = 0, \quad M_y = B_{26}(u,y + v,x + w,x w,y) - D_{12}w,xx - D_{22}w,yy = 0$$

$$u_0 = 0, \quad N_{xy} = A_{66}(u,y + v,x + w,x w,y) - B_{16}w,xx - B_{26}w,yy = 0$$

(3.2)

It may be noted that the displacement components given by Eqs.(2.9) and (2.10) satisfy the essential as well as the natural boundary conditions.

The results presented in Figs 3.1-3.29 are in following order :

Figs. 3.1-3.3 effect of the number of layers on the transverse deflection of square and rectangular plates with lamination angle 45° and fixed simple supports

Figs. 3.4-3.6 effect of the aspect ratio on the transverse deflection of plates with lamination angle 45° and fixed simple supports

Figs. 3.7-3.9 effect of the number of layers on the transverse deflection of square and rectangular plates with lamination angle 22.5° and fixed simple supports

Figs. 3.10-3.12 effect of the aspect ratio on the transverse deflection of plates with lamination angle 22.5° and fixed simple supports

Figs 3.13-3.21 effect of the lamination angle on the postbuckling response

Figs 3.22-3.25 effect of the number of layers and the aspect ratio on the transverse deflection of plates with sliding simple supports

Figs. 3.26-3.29 comparison of the effect of two types of boundary conditions on the postbuckling response

In Figs. 3.1-3.3, as the temperature increases from zero, the plate remains flat until the temperature reaches the critical value required for buckling. Beyond this temperature the deflection increases rapidly. It is noted that the critical temperature at which bifurcation (buckling) occurs increases with the increase in the number of layers. Moreover, the central deflection corresponding to a given temperature load decreases with increasing N . Since the coupling stiffnesses B_{16} and B_{26} can be shown to decrease with increasing N (see Appendix 2), it follows that membrane-twist coupling tends to increase the thermal lateral deflections. The difference between central deflections for $N=4$ and $N=6$ is very small; therefore, solutions corresponding to $N=4,6$ are close to the orthotropic solution. Hence, it follows that the effect of coupling stiffnesses is quite pronounced in $N=2$ case and it becomes less significant from $N=4$ onwards. For these laminates, the transverse displacement consists predominantly of mode (1,1) over the temperature range investigated; the next most

significant modes (1,3), (3,1) and (3,3) contribute only slightly to the lateral displacement. That is why, a rising trend in the central deflection is observed even at higher temperature loads, though at a reduced rate. This phenomenon is very clear for plates having the aspect ratio 1.5 and 2.0. As the aspect ratio increases the contribution of (1,3) mode to the central deflection increases. This explains the trend in Figs. 3.4-3.6, in which the central deflection of the plate having an aspect ratio 1.5 is less than that of plate with an aspect ratio 2.0 at small temperature loads. But at certain critical value of T/T^* , this trend is reversed. The central deflection of a square plate is always less when compared with the other two cases.

The effect of the number of layers on the postbuckling response of a plate with lamination angle 22.5° can be seen in Figs 3.7-3.9. In Fig. 3.7, it is noticed that beyond $T/T^* \approx 1.5$ the transverse deflection of a two-layer laminate is less than that of a four- and a six-layer laminate. The reason for this is that the mode changes from (1,1) to (1,3) mode. The change in mode shape is shown in 3-D plots (Figs 3.52 and 3.53). It is seen that the effect of (1,3) mode disappears as the number of layers increase from two to six. The effect of (1,3) mode in $N=6$ case can be seen only at initial temperature loads when it produces a kink in the curve. At higher temperature loads, only the (1,1) mode is dominant; the (1,3) mode contributes very

little to the central displacements. The variation of the lateral displacement at the center of the plate with different aspect ratio is shown in Figs. 3.10-3.12. From all these Figures it is observed that the plate having a higher aspect ratio deflects more but buckles at a lower temperature.

The central deflection and temperature relationships for two lamination angles considered are plotted in Figs 3.13-3.21. It is observed that the central deflection of a square laminate with lamination angle 22.5° is less when compared with the other case. But as the number of layers increase, the difference in the central plate deflection decreases and this becomes insignificant for $N=6$ (see Figs. 3.16 and 3.19). However, the reverse trend is observed in the case of rectangular plates. It is also found that the buckling temperature of a 45° laminate is always higher than that of a 22.5° laminate.

In Figs. 3.22-3.25, the response of antisymmetric angle-ply laminates with sliding simple supports is shown. Similar to the case of fixed simple supports, an increase in the number of layers results in a decrease in the central deflection of the plate. Again it is due to decrease of the coupling stiffnesses B_{16} and B_{26} . The postbuckling behaviour of antisymmetric angle-ply plates for different aspect ratio is given in Figs. 3.24-3.25. It found that the postbuckling strength decreases with an increase in the aspect ratio. For all these cases, the

mode shape (1,1) is predominant for the entire range of temperature considered.

The effect of inplane boundary conditions on the postbuckling response can be seen in the Figs 3.26-3.29. It is noted that the plate with fixed simple supports buckles at a lower temperature. The central deflection of square plates with sliding simple supports is always less than that of plate with fixed simple supports. But, in rectangular plates having sliding simple supports, the out-of-plane displacement at the center of plate is less when compared with fixed simple supports only up to certain temperature load. At higher temperature loads out-of-plane deflections at the center of plate are less for fixed simple supports. In the sliding simple supports, the postbuckling responses consist mainly of the deflections associated with the coefficient w_{11} . In the fixed simple supports, the plate buckles predominantly in the (1,1) mode. However, the deflection associated with w_{13} , begin to influence the postbuckling response more and more at higher temperatures in the rectangular plates.

Symmetric cross-ply laminates

Using Eq.(A1.14) of Appendix 1, it can be shown that for this case the thermal force N_{xy}^T and the thermal moments M_x^T , M_y^T , M_{xy}^T vanish. For this type of laminate boundary conditions become

Fixed simple supports:

along $x = 0, a$

$u_0 = 0, v_0 = 0, w = 0$ and

$$M_x = -D_{11}w_{,xx} - D_{12}w_{,yy} = 0$$

along $y = 0, b$

$u_0 = 0, v_0 = 0, w = 0$ and

$$M_y = -D_{12}w_{,xx} - D_{22}w_{,yy} = 0$$

(3.3)

The displacement components Eq. (2.9) satisfy the essential as well as the natural boundary conditions.

Figs 3.30-3.32 show central deflection versus temperature relationships for symmetric cross-ply laminates. It is noted that the postbuckling strength of laminate decreases with the increase in the aspect ratio of the plate. The effect of the number of layers is shown in Figs. 3.31 and 3.32.

Antisymmetric cross-ply laminates

For this type of laminates N_{xy}^T and M_{xy}^T are zero. Therefore, the boundary conditions become

Fixed simple supports:

along $x = 0, a$

$u_0 = 0, v_0 = 0, w = 0$ and

$$M_x = B_{11}(u,x + 1/2(w,x)^2) - D_{11}w,xx - D_{12}w,yy - M_x^T = 0$$

along $y = 0, b$

$u_0 = 0, v_0 = 0, w = 0$ and

$$M_y = B_{22}(v,y + 1/2(w,y)^2) - D_{12}w,xx - D_{22}w,yy - M_y^T = 0$$

(3.4)

Sliding simple supports:

along $x = 0, a$

$$w = 0, \quad M_x = B_{11}(u,x + 1/2(w,x)^2) - D_{11}w,xx - D_{12}w,yy - M_x^T = 0$$

$$u_0 = 0, \quad N_{xy} = A_{66}(u,y + v,x + w,x w,y) = 0$$

along $y = 0, b$

$$w = 0, \quad M_y = B_{22}(v,y + 1/2(w,y)^2) - D_{12}w,xx - D_{22}w,yy - M_y^T = 0$$

$$v_0 = 0, \quad N_{xy} = A_{66}(u,y + v,x + w,x w,y) = 0$$

(3.5)

In this case the assumed displacement components, expressed by Eqs.(2.9) and (2.10), satisfy the essential boundary conditions but not the natural boundary conditions. However, as in previous cases, nine terms in u and v displacement series and four terms in the w series are considered.

Figs 3.33-3.36 give transverse central deflections for square as well as rectangular cross-ply laminates. Unlike the cases considered earlier in which the simply supported laminates remain flat until the bifurcation (buckling) occurs, the antisymmetric cross-ply laminate deflects laterally immediately

upon loading. This unique behaviour of cross-ply can not be noticed by linear analysis (Thangaratnam, et al 1988). This behaviour is due to the presence of coupling stiffnesses B_{11} and B_{22} which couple normal moments with inplane compression. Fig 3.33 shows the effect of the number of layers on the transverse deflection of cross-ply laminates. It is observed that there is hardly any difference between the responses of four- and six-layer laminates. Since the coupling stiffnesses B_{11} and B_{22} can be shown to increase with decreasing N , it follows that B_{11} and B_{22} tend to increase deflections. In rectangular plates ($a/b = 2.0$, see Fig. 3.36), a two-layer laminate buckles in (1,1) mode but (1,3) mode begins to influence the response more and more as w_{13} approaches the magnitude of w_{11} . At a specific temperature the central deflection of a two-layer laminate becomes less than that of a four-layer laminate. Here at this point it can be noticed that in the case of four-layer laminate, the curve has a rising trend due to the presence of mode (1,1) only. Figs 3.34 and 3.35 show the effect of the aspect ratio on the central deflection of the plate.

Figs. 3.37-3.40 depict the nonlinear response of cross-ply laminates with sliding simple supports (type 2 boundary condition). Comparative study of the influence of two different boundary conditions is given in Figs. 3.41 and 3.42. It is observed that plates with the fixed simple supports deflect

out-of-plane more than plates with the sliding simple supports.

Angle-ply Vs. Cross-ply laminates

On the basis of the study carried out for antisymmetric angle-ply and cross-ply laminates the following points are observed :

- (i) The most interesting difference in the behaviour of two types of laminates is that the cross-ply laminates deflect out-of-plane as soon as thermal loads are applied, whereas angle-ply laminates remain flat till a critical temperature is reached after which the deflection increases rapidly with rise in temperature. In other words, bifurcation type of instability (buckling) is not observed in the case of antisymmetric cross-ply laminates.
- (ii) Out-of-plane deflection at the center of plate does not depend significantly on the number of lay-ups beyond $N=4$ in both angle- and cross-ply laminates (Figs. 3.1 and 3.33).
- (iii) The central deflection increases with the increase in the aspect ratio in both the cases considered but mode shape may influence the central deflection of the plate (see Figs. 3.5 and 3.39).
- (iv) The effect of inplane boundary conditions on the transverse deflection is much more pronounced in the case of cross-ply laminates, where it can be observed that that the plates with

the sliding simple supports are stiffer compared to the plates with the fixed simple supports (Figs 3.41 and 3.42). Antisymmetric angle-ply laminates do not show any significant difference in the lateral deflections for the two boundary conditions considered (Figs. 3.26 and 3.29).

3.3 NON-UNIFORM TEMPERATURE RESPONSE

Figs 3.43 to 3.51 show the response of antisymmetric angle-ply laminates in the presence of thermal gradient through-the-thickness of the plate. It is found that the plate undergoes lateral deflection as soon as the temperature is increased above the ambient temperature. However, for both sets of boundary conditions the deflections prior to the critical buckling temperature are very small and at only slightly higher temperature, the response becomes very close to the corresponding postbuckling response in the uniform temperature case. The effect of the number of layers on the out-of-plane deflections in the presence of slight thermal gradient is also studied. It is noticed that the response with higher number of layers is even closer to the postbuckling response of the earlier case. Therefore, it appears reasonable to conclude that a slight temperature gradient through-the-thickness of plate does not make much difference in the nonlinear response of the plate. A similar observation has also been reported recently by

Meyers and Heyer (1992).

It is further observed that the response of the plate with different fiber orientations in the presence of the temperature gradient is same as when the temperature is uniform, except that initial out-of-plane deflections are observed in the temperature-gradient case (Figs. 3.43-3.48). Again, the central deflection of the square plate with lamination angle 22.5° is less when compared with the case of lamination angle 45° . But as the number of lay-ups N increase, the difference in the out-of-plane displacement at the center of the plate decreases for the two cases and this difference become insignificant for $N=6$ (Figs. 3.45 and 3.48). The effect of inplane boundary conditions can be seen in Figs. 3.43-3.45 and Figs. 3.49-3.51. Here it is again noted that the central deflection of a square plate with sliding simple supports (type 2) is always less than that of a plate with fixed simple supports (type 1). Although the results for rectangular plates are not given here but it has been verified that their general response is similar to that for uniform temperature case except for the out-of-plane deflections setting in as soon as thermal loads are applied.

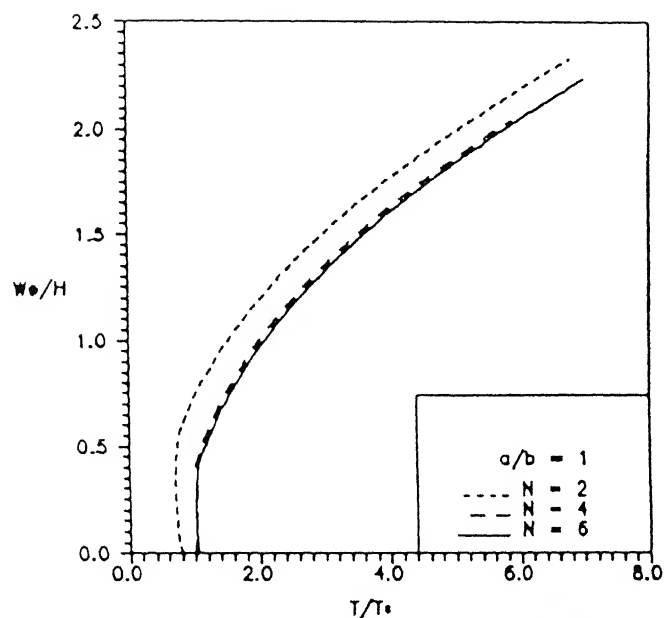


Fig. 3.1 Center deflection of antisymmetric angle-ply ($\Theta=45^\circ$) subjected to uniform temperature, Boundary condition: Type 1

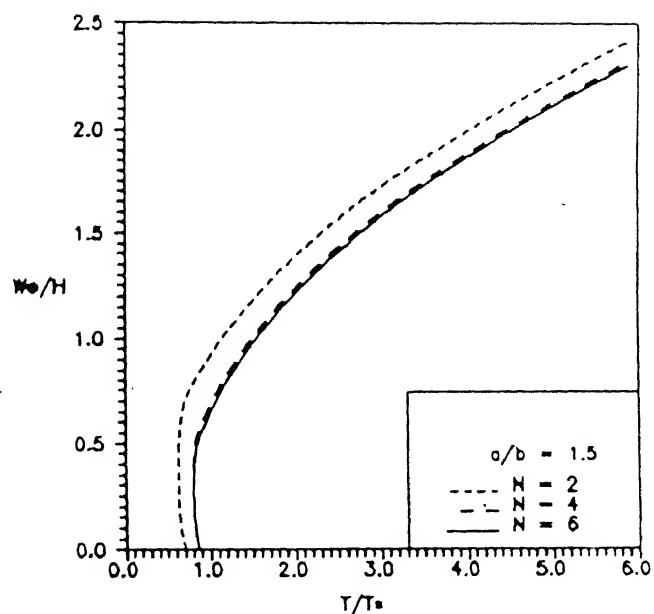


Fig. 3.2 Center deflection of antisymmetric angle-ply ($\Theta=45^\circ$) subjected to uniform temperature, Boundary conditions: Type 1

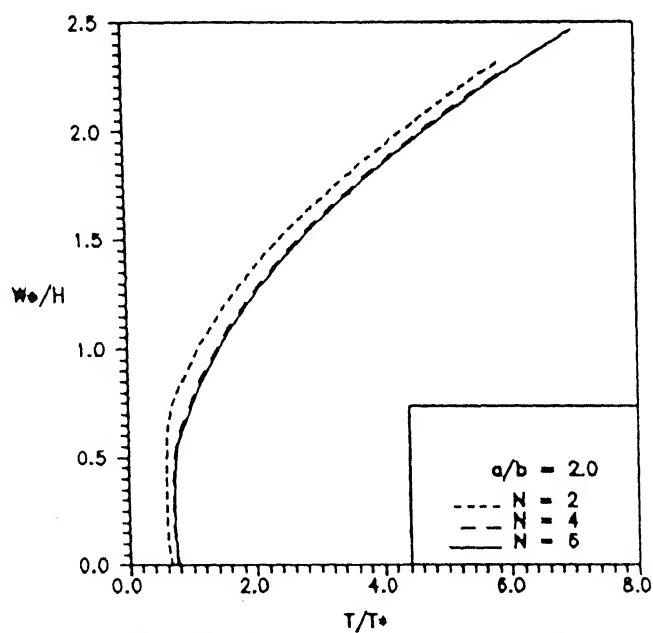


Fig. 3.3 Center deflection of antisymmetric angle-ply ($\Theta=45^\circ$) subjected to uniform temperature, Boundary conditions: Type 1

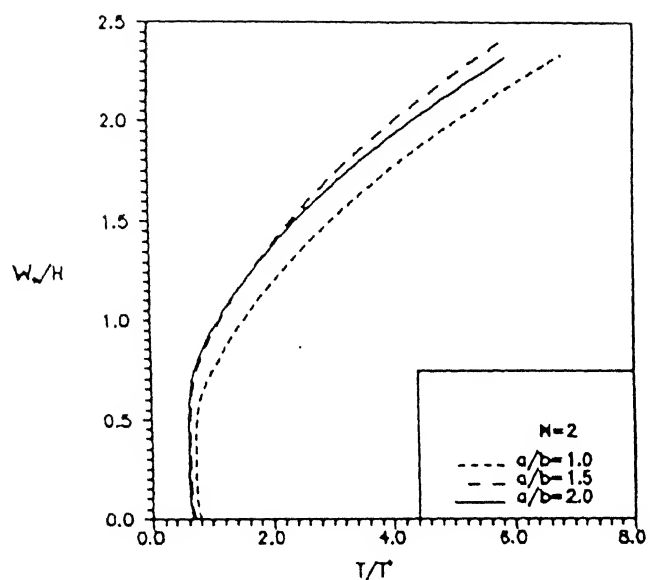


Fig. 3.4 Center deflection of antisymmetric angle-ply ($\Theta=45^\circ$) subjected to uniform temperature, Boundary conditions: Type 1

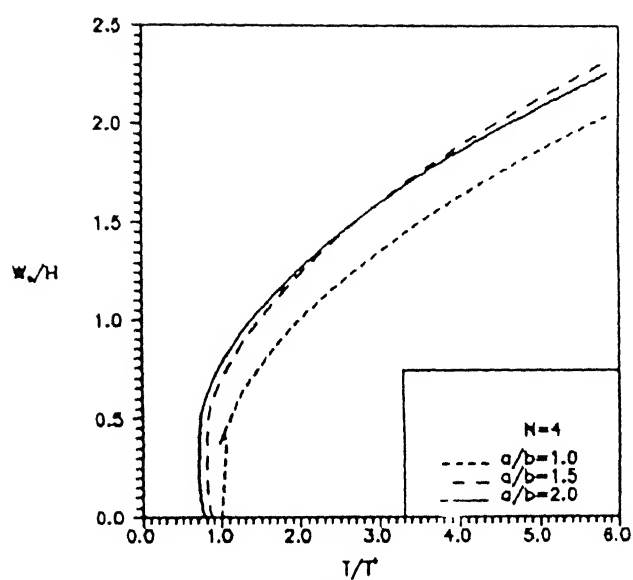


Fig. 3.5 Center deflection of antisymmetric angle-ply ($\Theta=45^\circ$) subjected to uniform temperature, Boundary conditions: Type 1

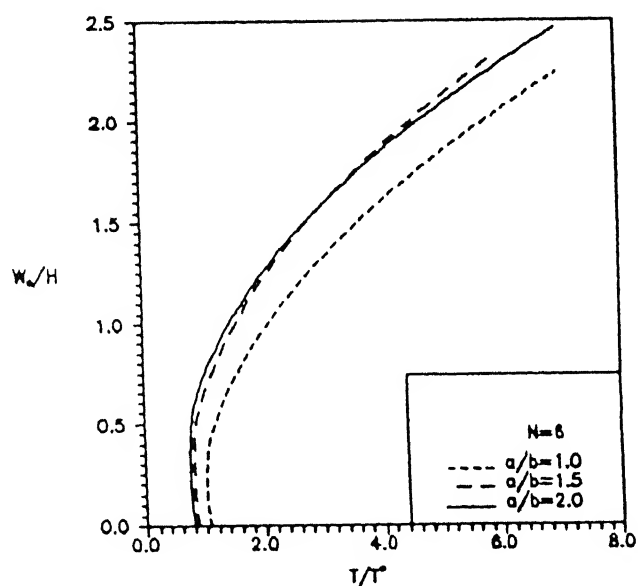


Fig. 3.6 Center deflection of antisymmetric angle-ply ($\Theta=45^\circ$) subjected to uniform temperature, Boundary conditions: Type 1

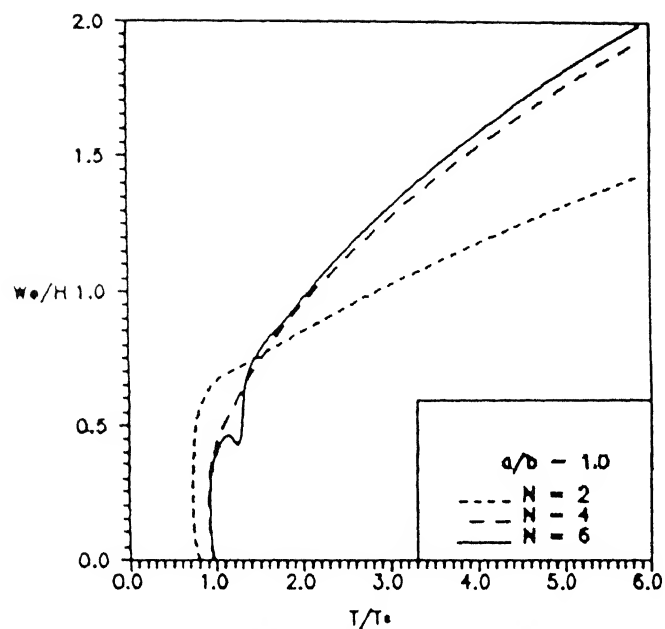


Fig. 3.7 Center deflection of antisymmetric angle-ply ($\Theta=22.5^\circ$) subjected to uniform temperature, Boundary conditions: Type 1

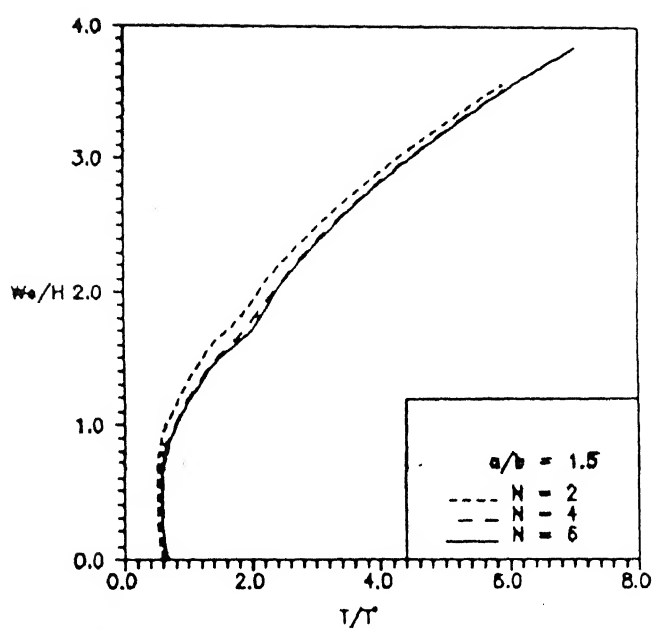


Fig. 3.8 Center deflection of antisymmetric angle-ply ($\Theta=22.5^\circ$) subjected to uniform temperature, Boundary conditions: Type 1

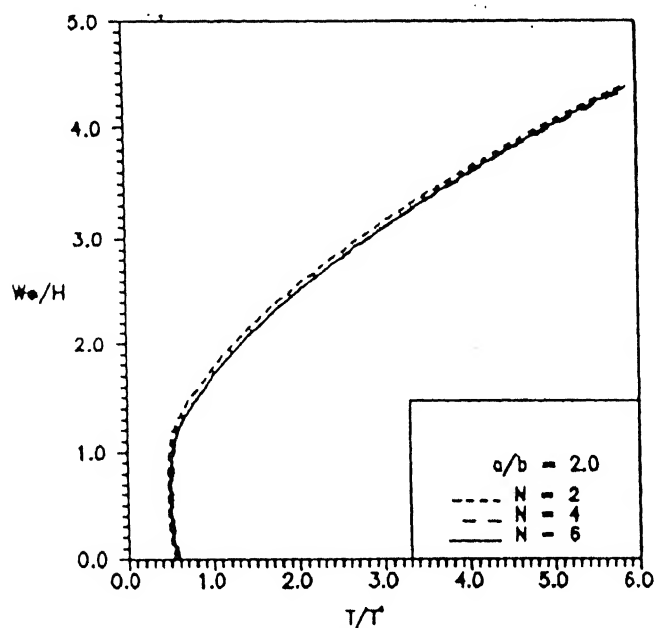


Fig. 3.9 Center deflection of antisymmetric angle-ply ($\Theta=22.5^\circ$) subjected to uniform temperature, Boundary conditions: Type 1

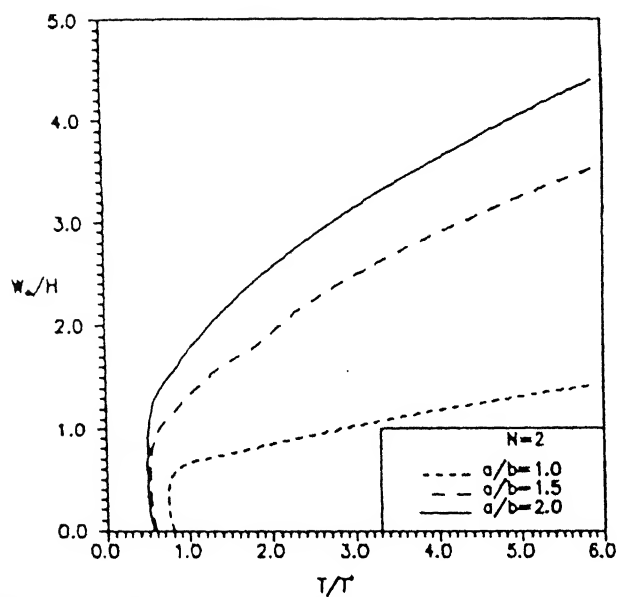


Fig. 3.10 Center deflection of antisymmetric angle-ply ($\Theta=22.5^\circ$) subjected to uniform temperature, Boundary conditions: Type 1

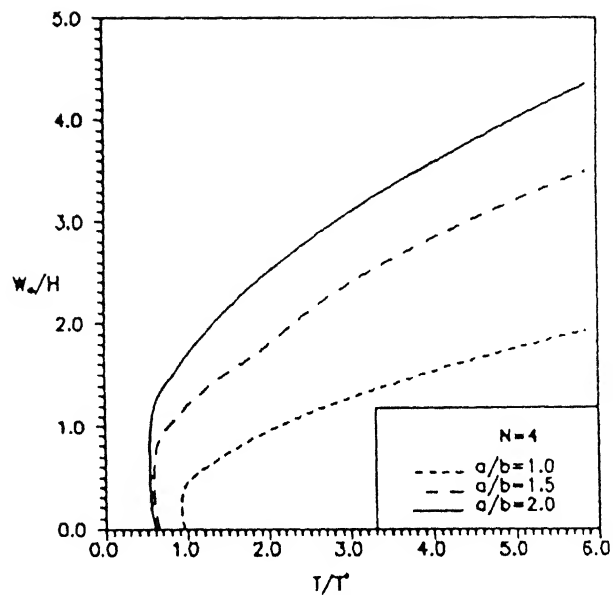


Fig. 3.11 Center deflection of antisymmetric angle-ply ($\Theta=22.5^\circ$) subjected to uniform temperature, Boundary conditions: Type 1

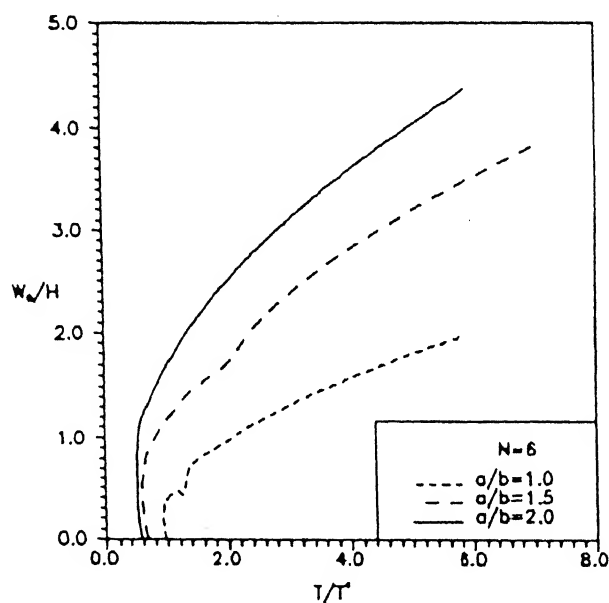


Fig. 3.12 Center deflection of antisymmetric angle-ply ($\Theta=22.5^\circ$) subjected to uniform temperature, Boundary conditions: Type 1

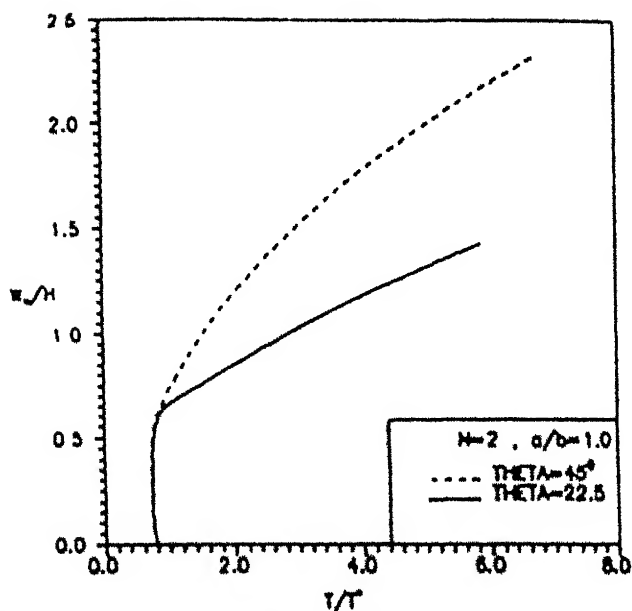


Fig. 3.13 Center deflection of antisymmetric angle-ply subjected to uniform temperature
Boundary conditions: Type 1

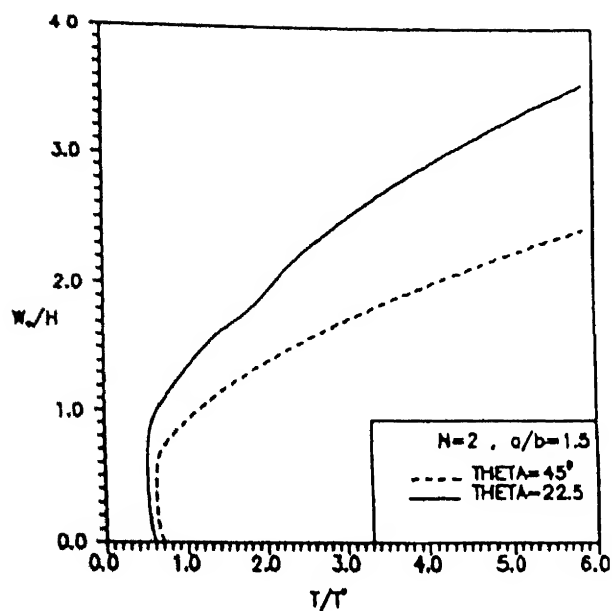


Fig. 3.14 Center deflection of antisymmetric angle-ply subjected to uniform temperature
Boundary conditions: Type 1

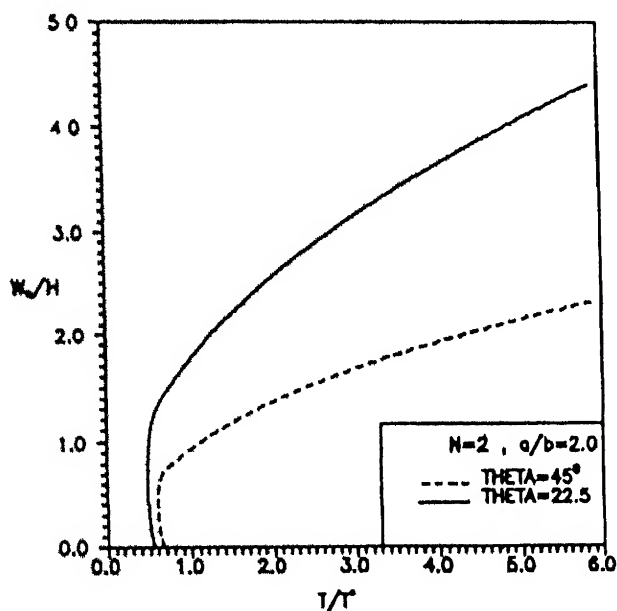


Fig. 3.15 Center deflection of antisymmetric angle-ply subjected to uniform temperature
Boundary conditions: Type 1

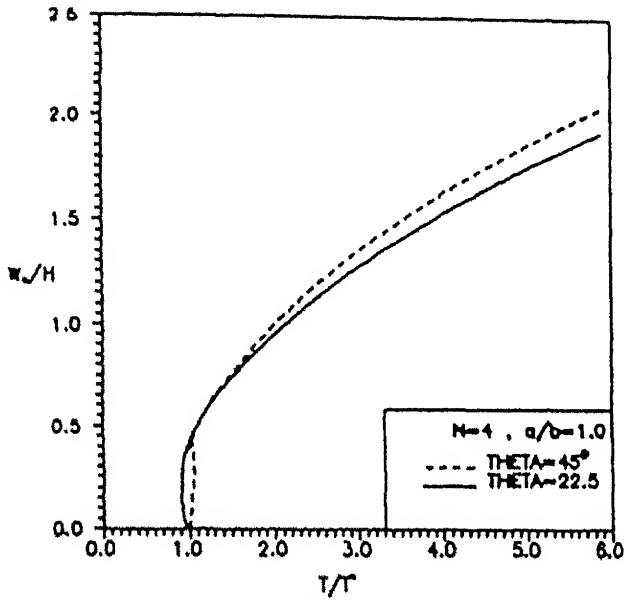


Fig. 3.16 Center deflection of antisymmetric angle-ply subjected to uniform temperature Boundary conditions: Type 1

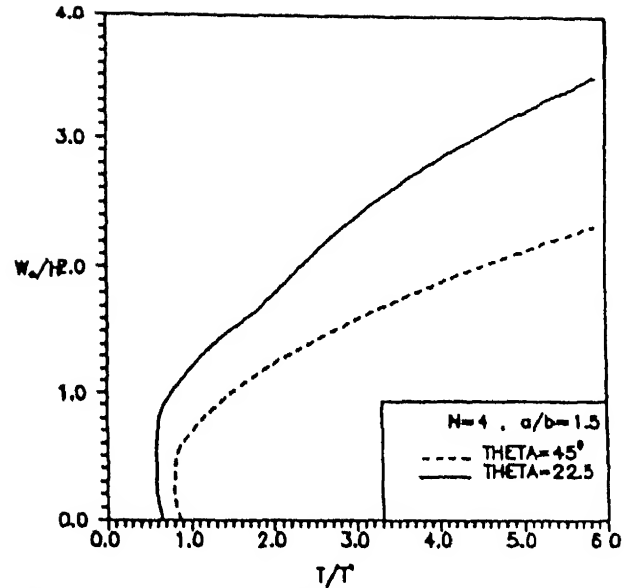


Fig. 3.17 Center deflection of antisymmetric angle-ply subjected to uniform temperature Boundary conditions: Type 1

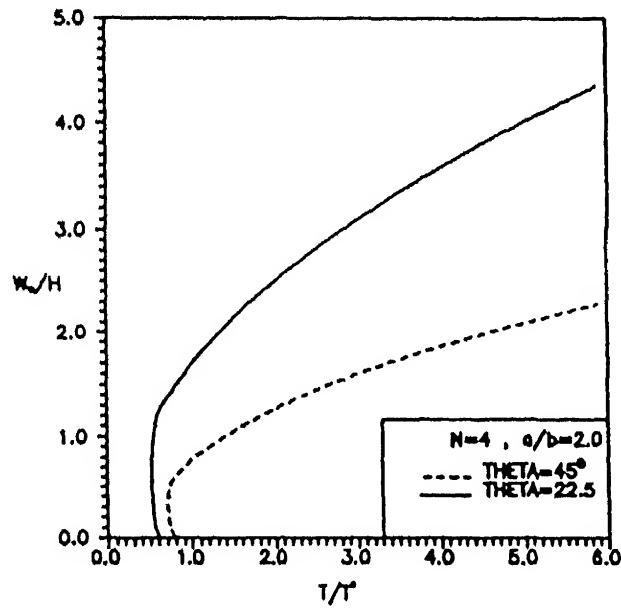


Fig. 3.18 Center deflection of antisymmetric angle-ply subjected to uniform temperature Boundary conditions: Type 1

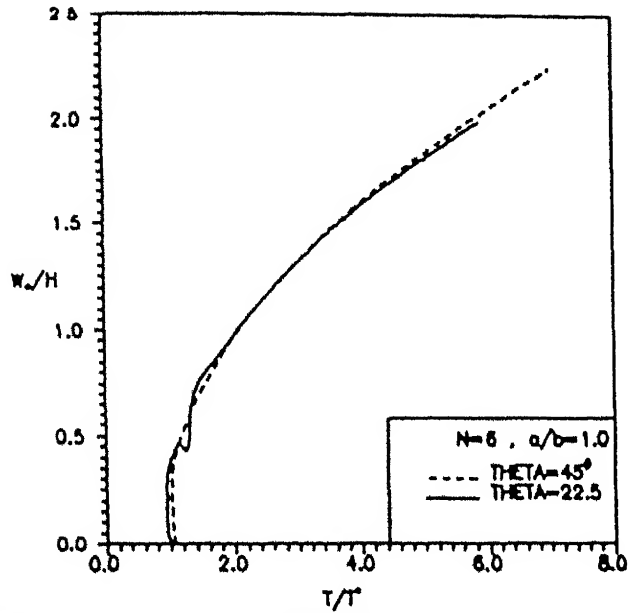


Fig. 2.19 Center deflection of antisymmetric angle-ply subjected to uniform temperature
Boundary conditions: Type 1

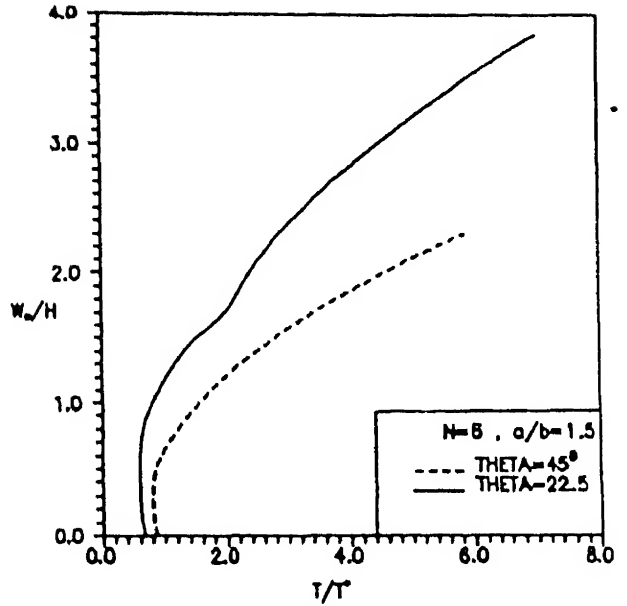


Fig. 2.20 Center deflection of antisymmetric angle-ply subjected to uniform temperature
Boundary conditions: Type 1

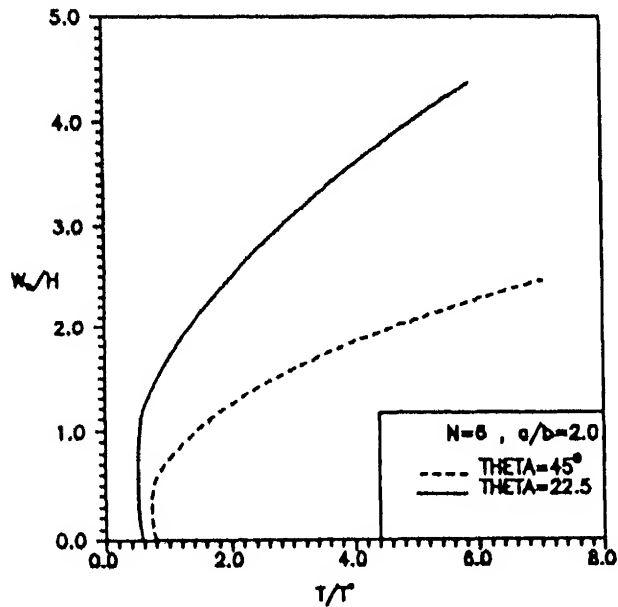


Fig. 2.21 Center deflection of antisymmetric angle-ply subjected to uniform temperature
Boundary conditions: Type 1

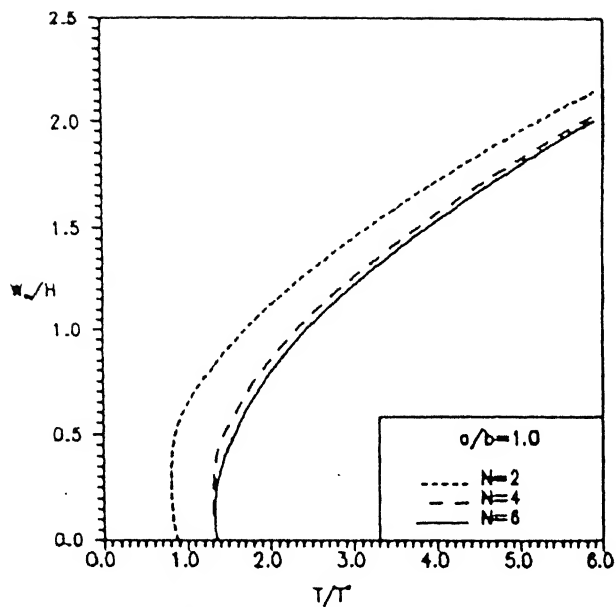


Fig. 3.22 Center deflection of antisymmetric angle-ply ($\Theta=45^\circ$) subjected to uniform temperature, Boundary conditions: Type 2

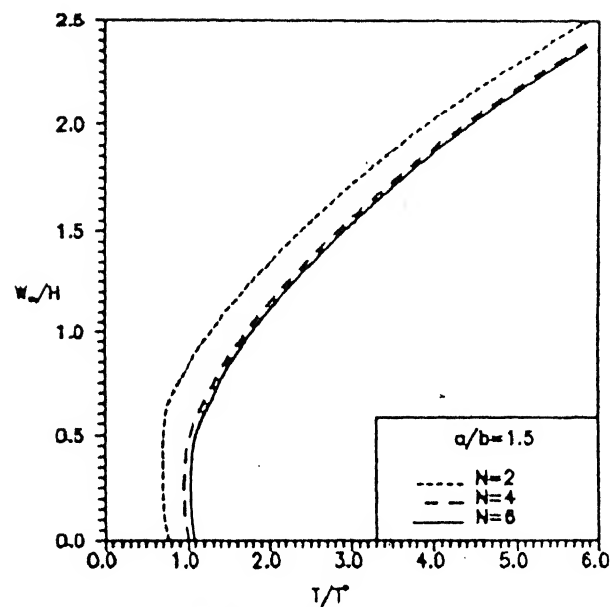


Fig. 3.23 Center deflection of antisymmetric angle-ply ($\Theta=45^\circ$) subjected to uniform temperature, Boundary conditions: Type 2

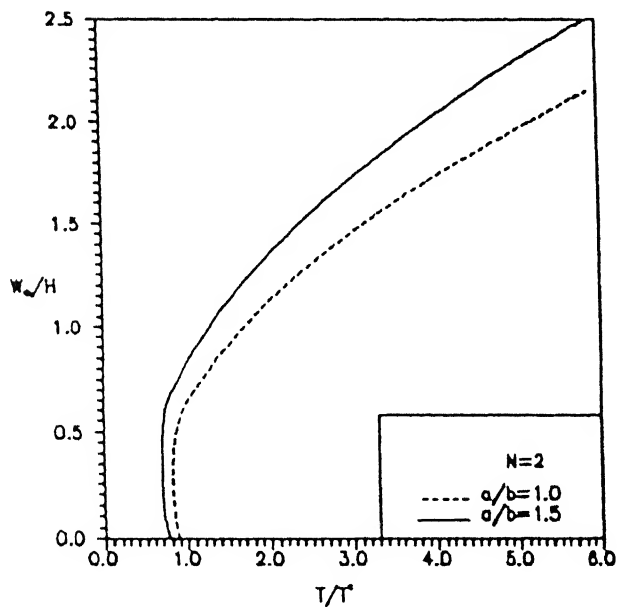


Fig. 3.24 Center deflection of antisymmetric angle-ply ($\Theta=45^\circ$) subjected to uniform temperature, Boundary conditions: Type 2

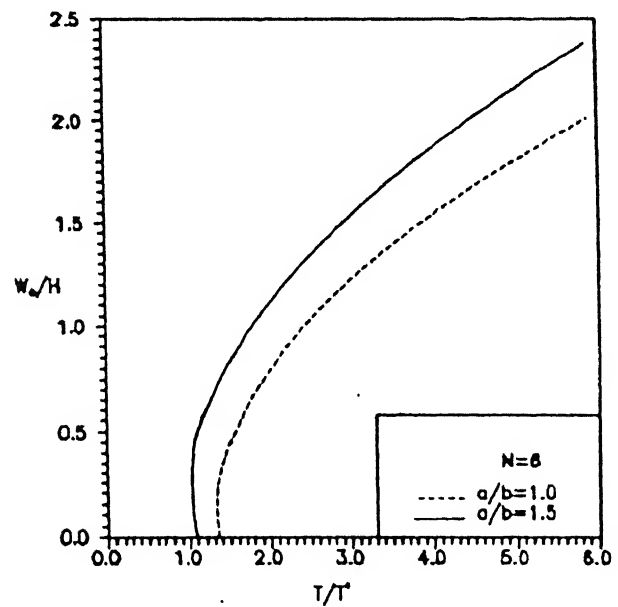


Fig. 3.25 Center deflection of antisymmetric angle-ply ($\Theta=45^\circ$) subjected to uniform temperature, Boundary conditions: Type 2

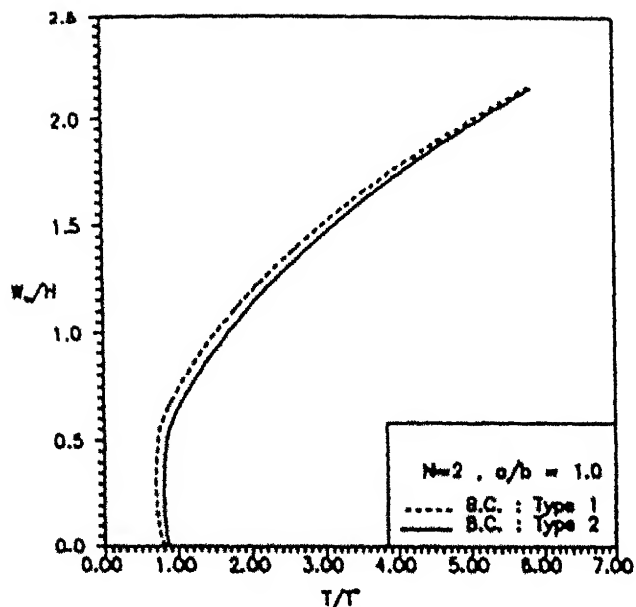


Fig. 3.26 Center deflection of antisymmetric glass-ply ($\Theta=45^\circ$) subjected to uniform temperature

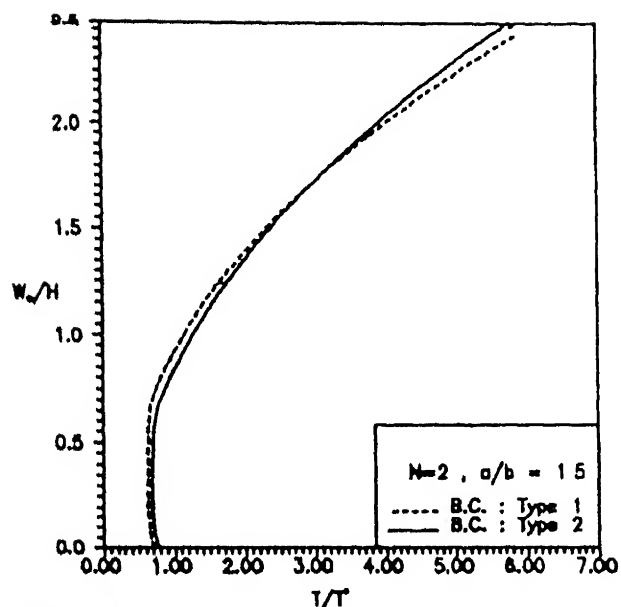


Fig. 3.27 Center deflection of antisymmetric angle-ply ($\Theta=45^\circ$) subjected to uniform temperature

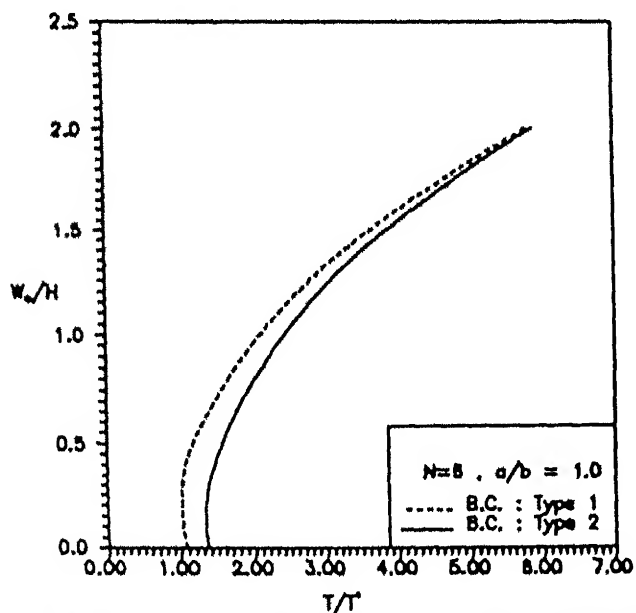


Fig. 3.28 Center deflection of antisymmetric glass-ply ($\Theta=45^\circ$) subjected to uniform temperature

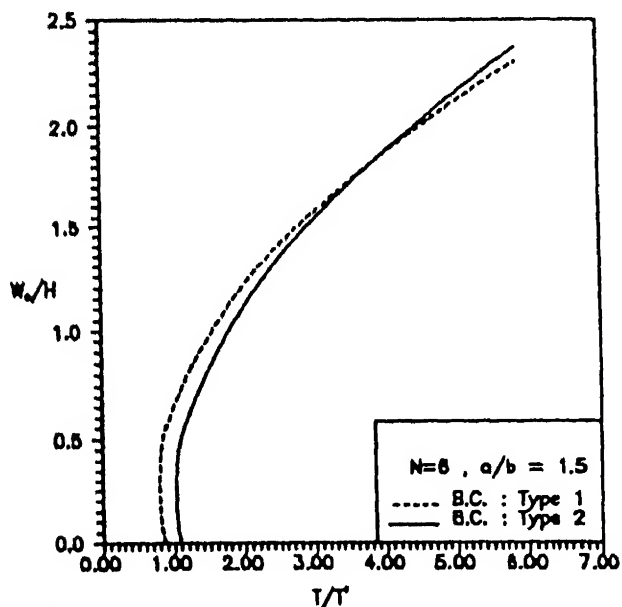


Fig. 3.29 Center deflection of antisymmetric angle-ply ($\Theta=45^\circ$) subjected to uniform temperature

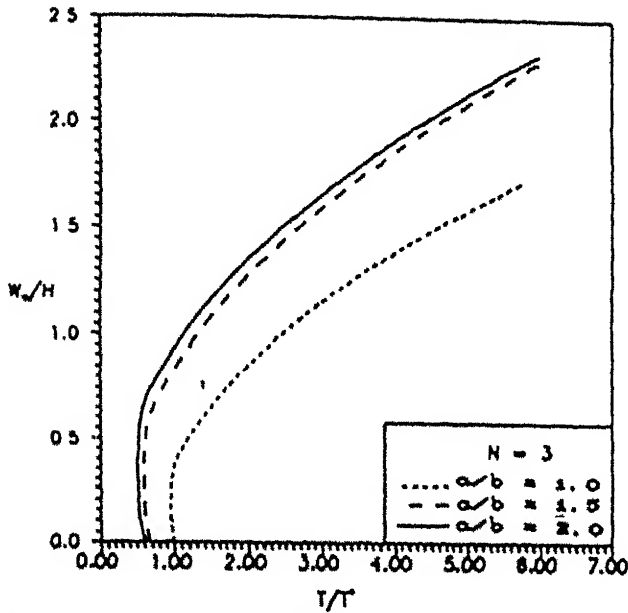


Fig. 3.20 Center deflection of symmetric cross-ply subjected to uniform temperature
Boundary conditions : Type 1

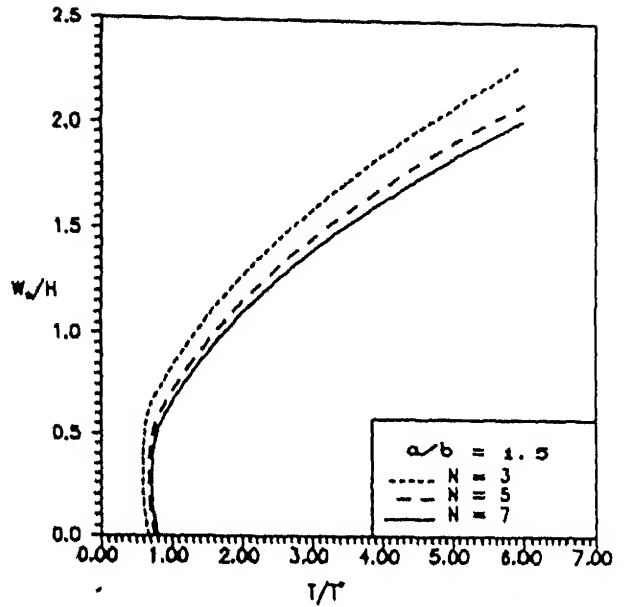


Fig. 3.21 Center deflection of symmetric cross-ply subjected to uniform temperature
Boundary conditions : Type 1

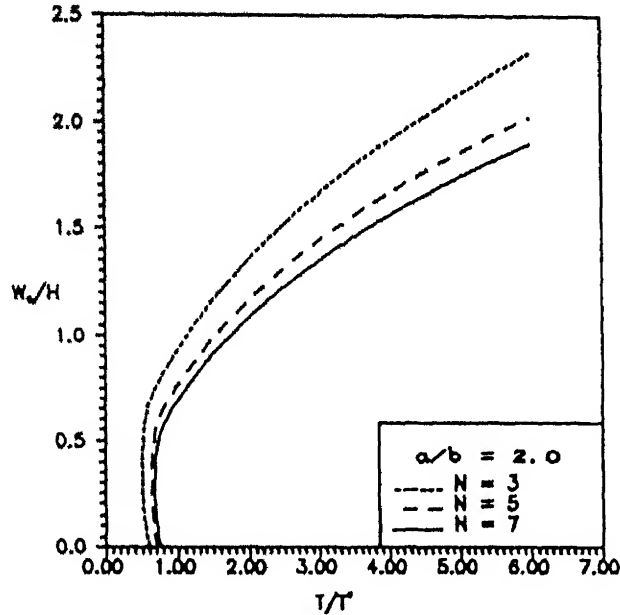


Fig. 3.22 Center deflection of symmetric cross-ply subjected to uniform temperature
Boundary conditions : Type 1

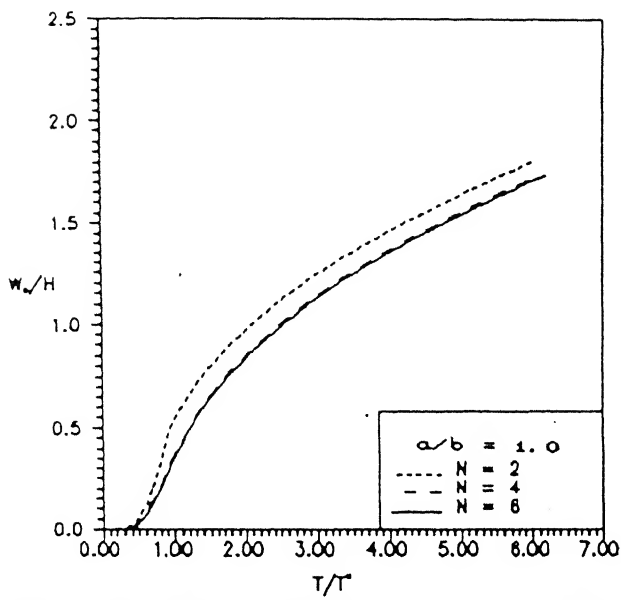


Fig. 3.33 Center deflection of antisymmetric cross-ply subjected to uniform temperature
Boundary conditions : Type 1

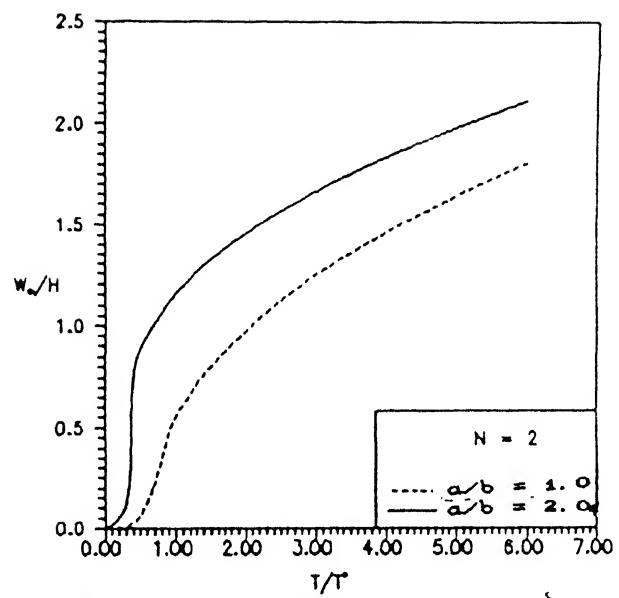


Fig. 3.34 Center deflection of antisymmetric cross-ply subjected to uniform temperature
Boundary conditions : Type 1

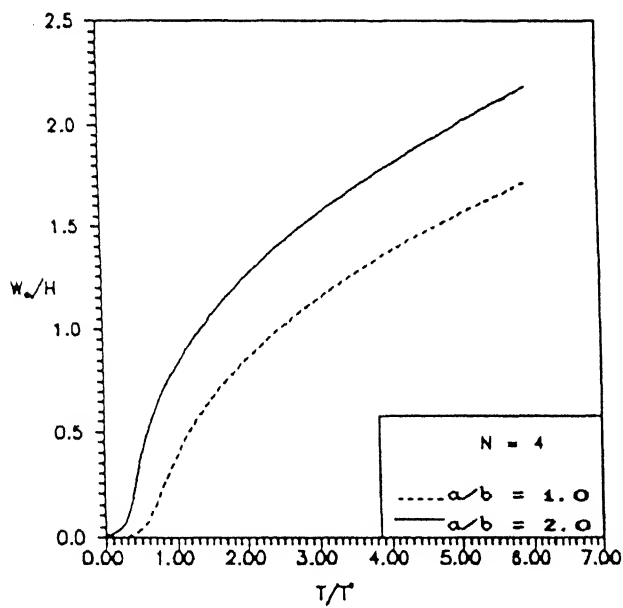


Fig. 3.35 Center deflection of antisymmetric cross-ply subjected to uniform temperature
Boundary conditions : Type 1

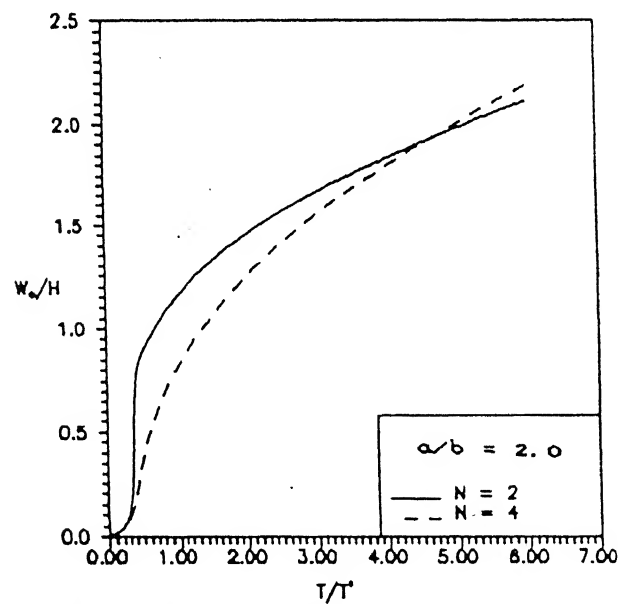


Fig. 3.36 Center deflection of antisymmetric cross-ply subjected to uniform temperature
Boundary conditions : Type 1

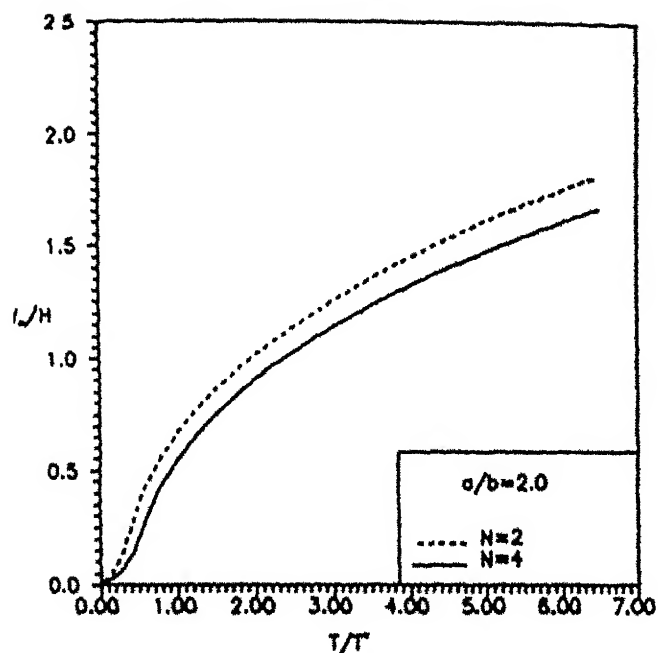


Fig. 3.37 Center deflection of antisymmetric cross-ply subjected to uniform temperature boundary conditions : Type 2

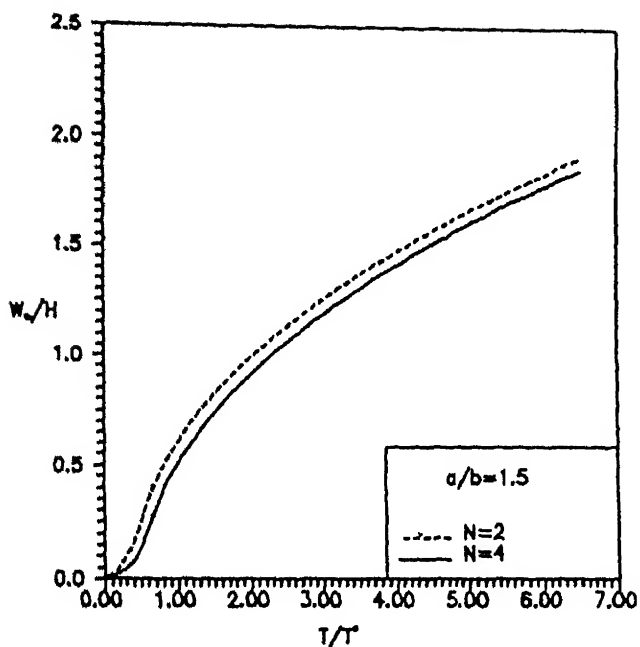


Fig. 3.38 Center deflection of antisymmetric cross-ply subjected to uniform temperature boundary conditions : Type 2

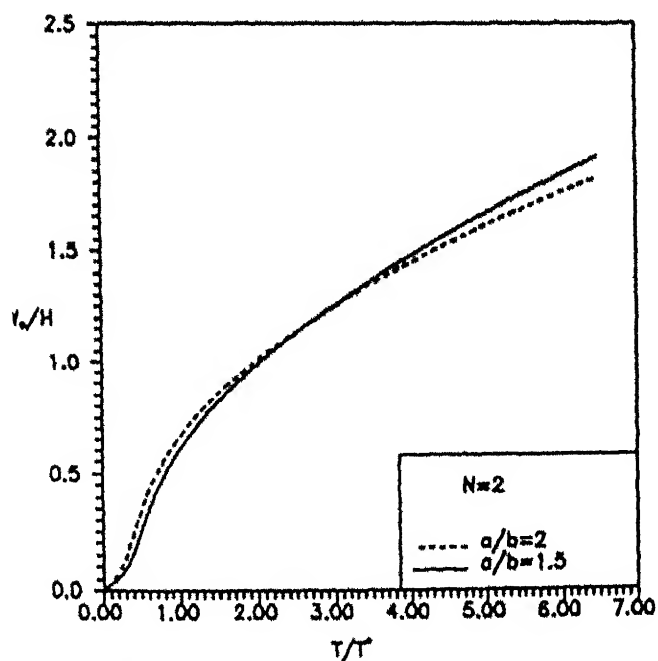


Fig. 3.39 Center deflection of antisymmetric cross-ply subjected to uniform temperature boundary conditions : Type 2

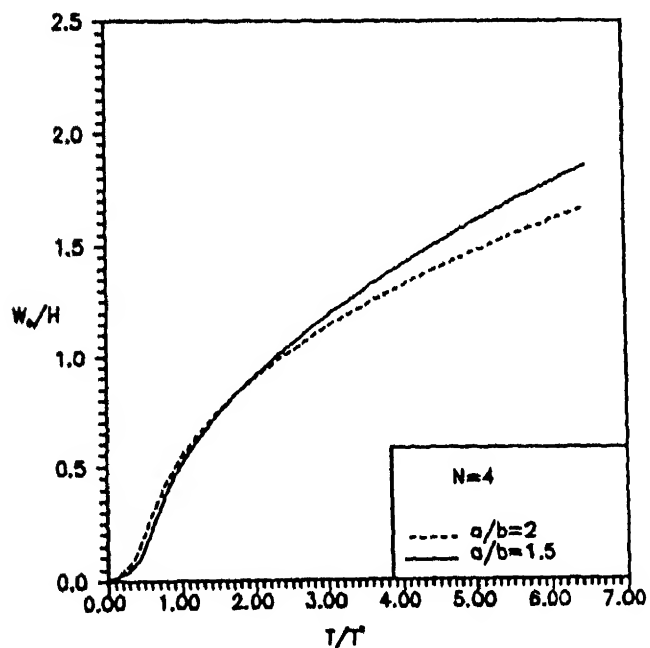


Fig. 3.40 Center deflection of antisymmetric cross-ply subjected to uniform temperature boundary conditions : Type 2

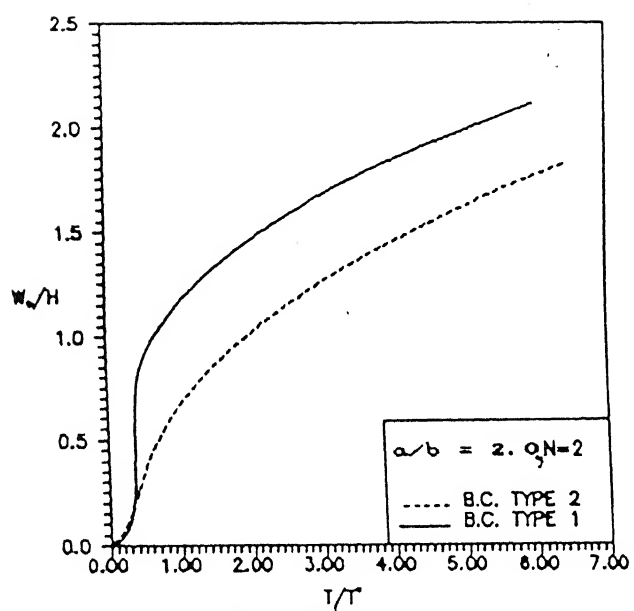


Fig. 2.41 Center deflection of antisymmetric cross-ply subjected to uniform temperature

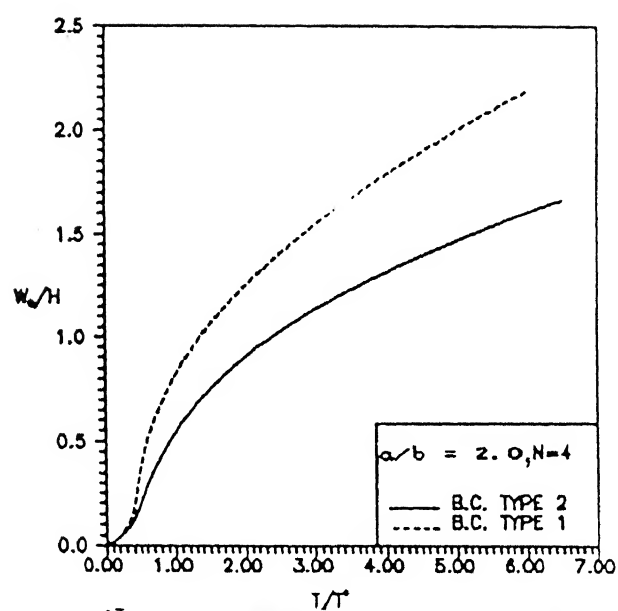


Fig. 3.42 Center deflection of antisymmetric cross-ply subjected to uniform temperature

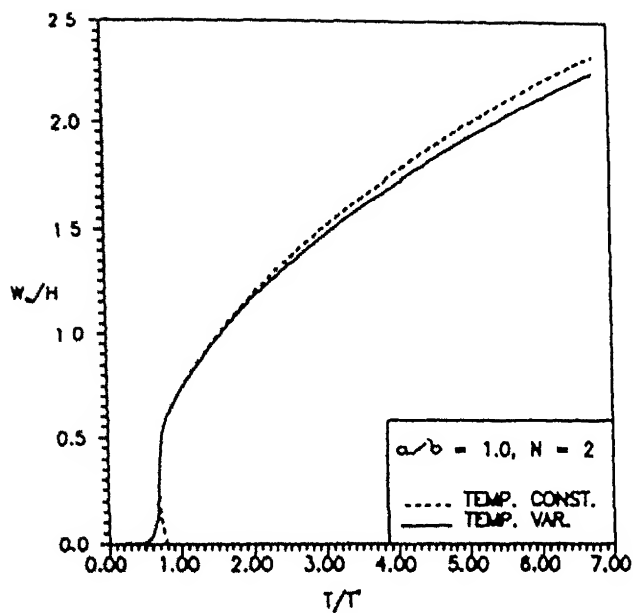


Fig. 2.42 Center deflection of antisymmetric angle-ply ($\Theta=45^\circ$), boundary conditions : Type 1

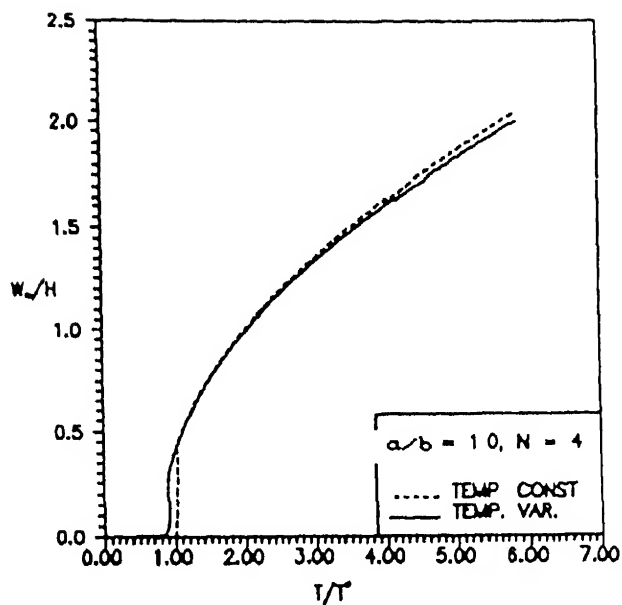


Fig. 2.44 Center deflection of antisymmetric angle-ply ($\Theta=45^\circ$), boundary conditions : Type 1

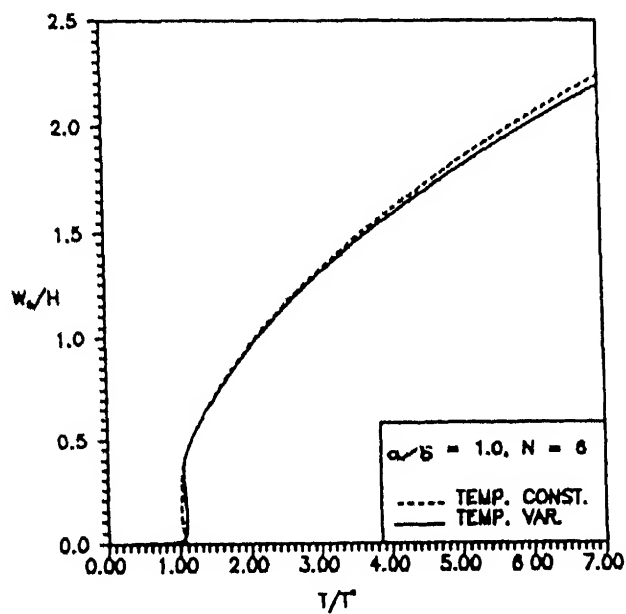


Fig. 2.45 Center deflection of antisymmetric angle-ply ($\Theta=45^\circ$), boundary conditions : Type 1

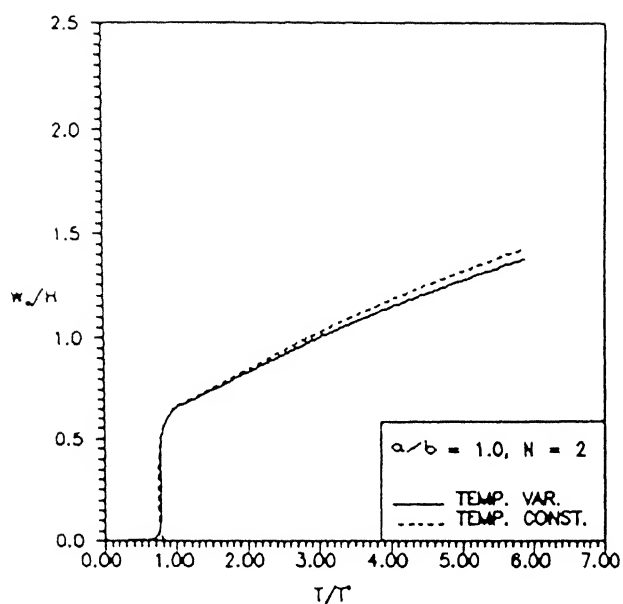


Fig. 3.46 Center deflection of antisymmetric angle-ply ($\Theta=22.5^\circ$), boundary conditions : Type 1

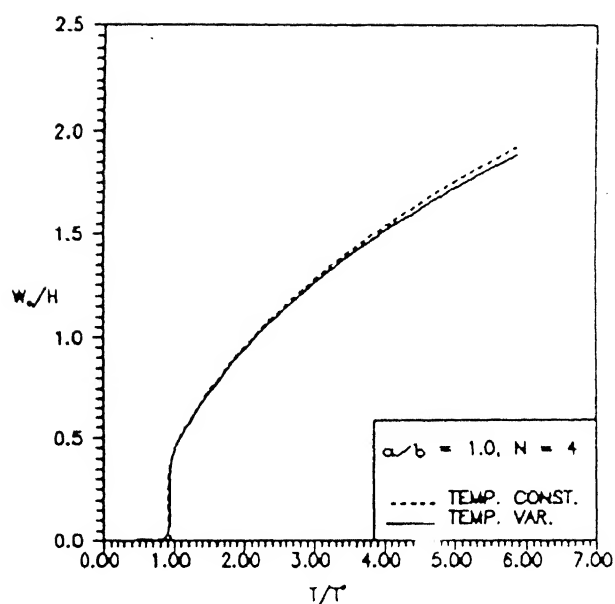


Fig. 3.47 Center deflection of antisymmetric angle-ply ($\Theta=22.5^\circ$), boundary conditions : Type 1

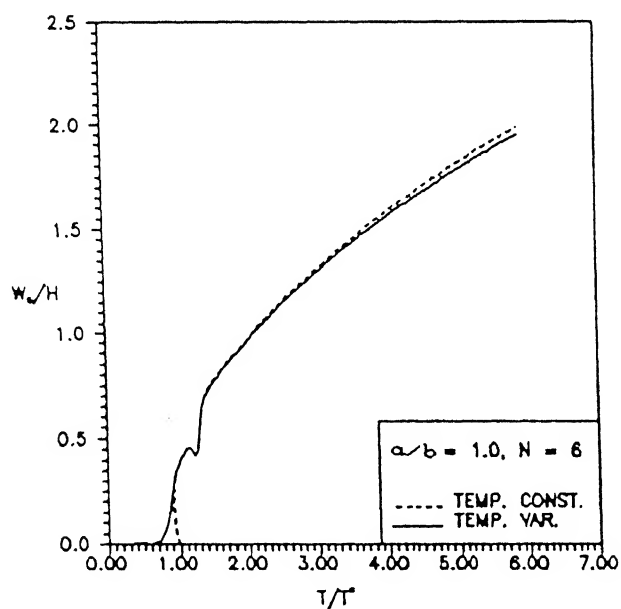


Fig. 3.48 Center deflection of antisymmetric angle-ply ($\Theta=22.5^\circ$), boundary conditions : Type 1

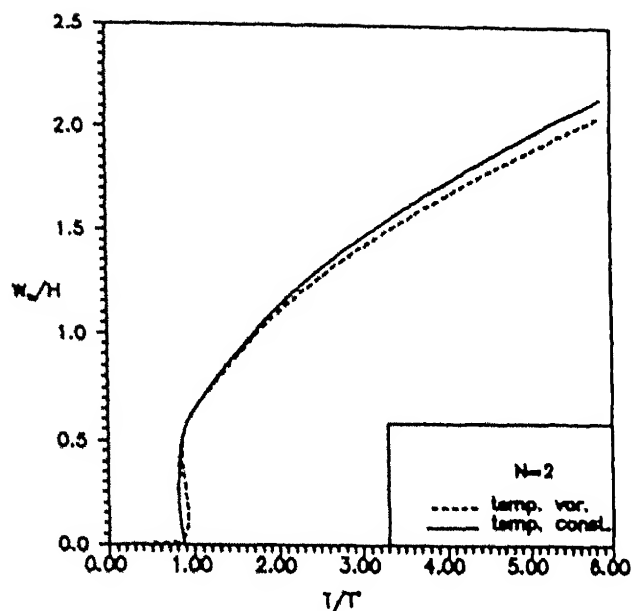


Fig. 2.49 Center deflection of antisymmetric angle-ply ($\Theta=45^\circ$), boundary conditions : Type 2

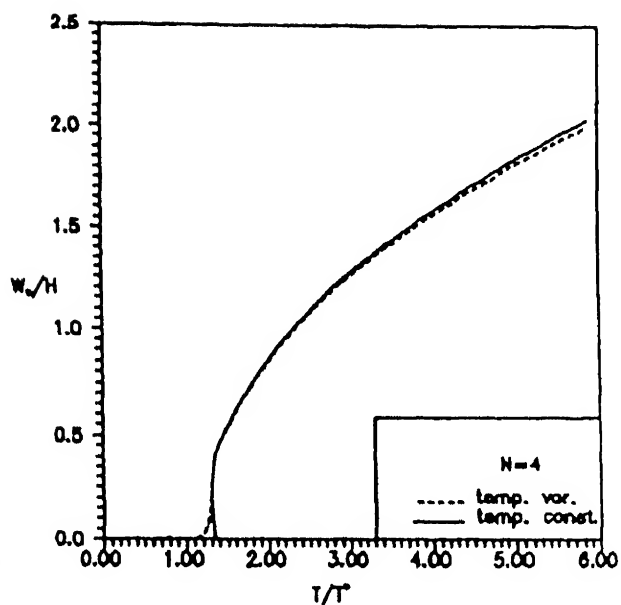


Fig. 2.50 Center deflection of antisymmetric angle-ply ($\Theta=45^\circ$), boundary conditions : Type 2

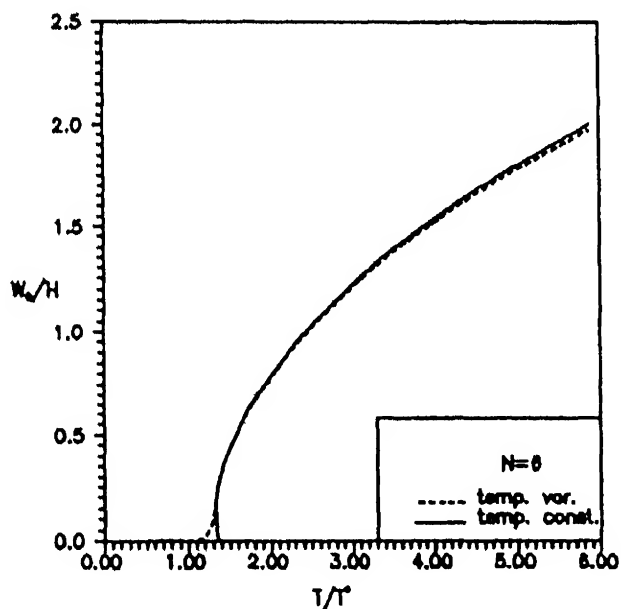


Fig. 2.51 Center deflection of antisymmetric angle-ply ($\Theta=45^\circ$), boundary conditions : Type 2

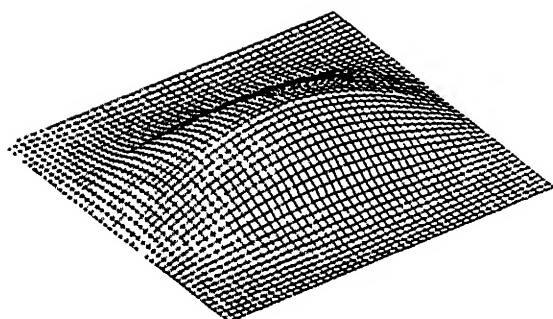


Fig. 2.52 Deflected shape just beyond buckling of a laminate ($\theta = 22.5^\circ$, $a/b = 1.0$, $N = 2$) subjected to uniform temperature.

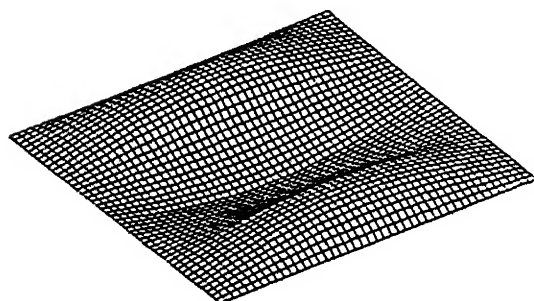


Fig. 3.52 Deflected shape of a laminate ($\theta = 22.5^\circ$, $a/b = 1.0$, $N = 2$) at $T/T^* \approx 5.0$

CONCLUSIONS

4.1 CONCLUDING REMARKS

The method of incremental thermal loads used in this investigation provides a means for studying moderately large deformation response of angle- and cross-ply laminated plates. Two types of inplane boundary conditions have been considered. The effect of imperfection in temperature field in the form of a slight temperature gradient through-the-thickness of the plate, has been considered.

On the basis of the limited study carried out the following conclusions can be drawn:

(i) The thermal postbuckling characteristics are significantly influenced by the number of layers. The effect of coupling stiffnesses B_{16} and B_{26} is quite pronounced in a two-layer case and it becomes less significant from the four-layer case onwards. The change in mode shape also plays very important role in determining the lateral displacement of the plate.

(ii) The thermal postbuckling strength decreases with the increase in the plate aspect ratio for angle-ply laminates and cross-ply laminated plates.

(iii) The magnitude of the transverse deflection at the center of the plate gets substantially changed by changing the lamination angle θ .

(iv) Support conditions can change the deflection response of the laminates. In general, plates with fixed simple supports deflect more than plates with sliding simple supports.

(v) Antisymmetric cross-ply laminates deflect out-of-plane immediately upon the application of thermal loads, i.e. the classical buckling is precluded in this case. This unique behaviour is due to presence of B_{11} and B_{22} terms in the coupling matrix.

(vi) The presence of small imperfection in the temperature, in the form of through-the-thickness gradient does not greatly affect nonlinear behaviour of laminates.

4.2 RECOMMENDATIONS FOR FUTURE WORK .

The formulation developed does not include transverse shear deformation effects. As a/H ratio becomes less than or equal to 20, the shear deformation effects become increasingly important. This aspect can be included in the analysis. Most of the studies carried out recently consider only lateral defections of the plate even at very high temperature loads. At that stage excessive stresses may cause delamination, cracks etc. Therefore, it is equally important to include stress analysis in the investigation. The combined effect of mechanic and thermal loads on the postbuckling response of laminate is also an important topic for study.

REFERENCES

- Agarwal, B. D. and Broutman, L. J. (1980). *Analysis and performance of fiber composites*. John Wiley & Sons.
- Banerjee and Datta (1979). Large deflections of elastic plates under nonstationary temperatures. *J. Eng. Mech. Div.*, 105, 705-711.
- Biswas, P. (1978a). Large deflection of heated cylindrical shells. *Int. J. Mech. Sci.*, 20, 17-20.
- Biswas, P. (1978b). Large deflections of heated orthotropic plates. *Indian J. Pure Appl. Math.*, 9, 1027-1032.
- Biswas, P. (1981). Nonlinear analysis of heated orthotropic plates. *Indian J. Pure Appl. Math.*, 12, 1380-1389.
- Chen, L. W. and Chen, L. Y. (1989). Thermal postbuckling analysis of laminated composites plates by finite element method. *Composite struc.* vol 12, 257-270.
- Chen, L. W. and Chen, L. Y. (1991). Thermal postbuckling behaviours of laminated composites plates with temperature dependent properties. *Composite struc.* vol 19, 267-283.
- Forray, M. and Newman, M. (1962a). On the postbuckling behaviour of rectangular plates. *J. Aero. Sci.*, 29, 754-755.
- Forray, M. and Newman, M. (1962b). The postbuckling analysis of heated rectangular plates. *J. Aero Sci.*, 29, 1262.
- Gossard, M. L., Siede, P. and Roberts, W. M. (1952). Thermal buckling of plates. *NACA, TN 2771*.
- Huang, N. N. and Tauchert, T. R. (1988a). Postbuckling response of antisymmetric angle-ply laminates subjected to uniform loading. *Acta Mechanica*, 72, 173-183.
- Huang, N. N. and Tauchert, T. R. (1988b). Large deflection of antisymmetric angle-ply laminates resulting from nonuniform temperature loadings. *J. Thermal stresses*, 11, 287-297.
- Huang, N. N. and Tauchert, T. R. (1991). Large deflection of laminated cylindrical and curved panels under thermal loading. *Computer & Structure* vol. 41, No. 2, 303-312.
- Jones, R. M. (1975). *Mechanics of composite Materials*. McGraw-Hill Kogakusha, Ltd.
- Mahayani, M. A. (1966). Thermal buckling of shallow shells. *Int. J. solids struct.*, 2, 167-180.

- Meyers, C. A and Heyer, M W. (1992). Thermally-induced, geometrically nonlinear response of symmetrically laminated composite plates. *Composite Engineering*, vol.2, No.1, 3-20.
- Prabhu, M. S. S. and Durvasula, S. (1976) Thermal postbuckling characteristics of clamped skew plates. *Computers & Structures*, 6, 177-185.
- Raju, K. K. and Rao, G. V. (1984). Thermal postbuckling of circular plates. *Computers & structures*, 18, 1179-1182.
- Thangaratnam, K. R. et al. (1988). Thermal buckling of composite laminated plates. *computer & structure*, vol. 32, No. 5, 1117-1124.
- Tauchert, T. R. and Huang, N. N. (1986). Thermal buckling and postbuckling behaviours of antisymmetric angle-ply laminates. *Proc. Int. Symp. on composites materials structures, Beijing*.
- Tauchert, T. R. (1991). Thermally-induced flexure, buckling and vibration of plates. *Appl. Mech. Rev.* vol 44, No. 8, 347-360.
- Wilcox, M. W. & Clemmer, L. E. (1964). Large deflection analysis of heated plates. *J. Eng. Mech. Div.*, 90, 165-189.

APPENDIX 1

1.1 STRESS-STRAIN RELATIONS FOR A LAMINA .

If the material axes are aligned with the natural body axes for the problem, then such lamina is called specially orthotropic lamina. Stress strain relations for such lamina under plane stress can be written as (Agarwal & Broutman 1980)

$$\begin{Bmatrix} \sigma_L \\ \sigma_T \\ \tau_{LT} \end{Bmatrix} = \begin{bmatrix} Q_{11} & Q_{12} & 0 \\ Q_{12} & Q_{22} & 0 \\ 0 & 0 & Q_{66} \end{bmatrix} \begin{Bmatrix} \epsilon_L \\ \epsilon_T \\ \gamma_{LT} \end{Bmatrix} \quad (A1.1)$$

where L and T subscripts refer to the longitudinal direction (L) and the transverse direction (T), respectively. [Q] is the reduced stiffness matrix and can be expressed in terms of engineering constants as under

$$\begin{aligned} Q_{11} &= E_L / (1 - \nu_{LT} \nu_{TL}) \\ Q_{22} &= E_T / (1 - \nu_{LT} \nu_{TL}) \\ Q_{12} &= \nu_{TL} E_L / (1 - \nu_{LT} \nu_{TL}) \\ Q_{66} &= G_{LT} \end{aligned} \quad (A1.2)$$

Here E_L , E_T are the elastic moduli in L and T directions (Fig A1.1), respectively, G_{LT} is the shear modulus in the L-T plane, ν_{LT} is the Poisson's ratio for transverse strain in the T-direction

when stressed in the L-direction

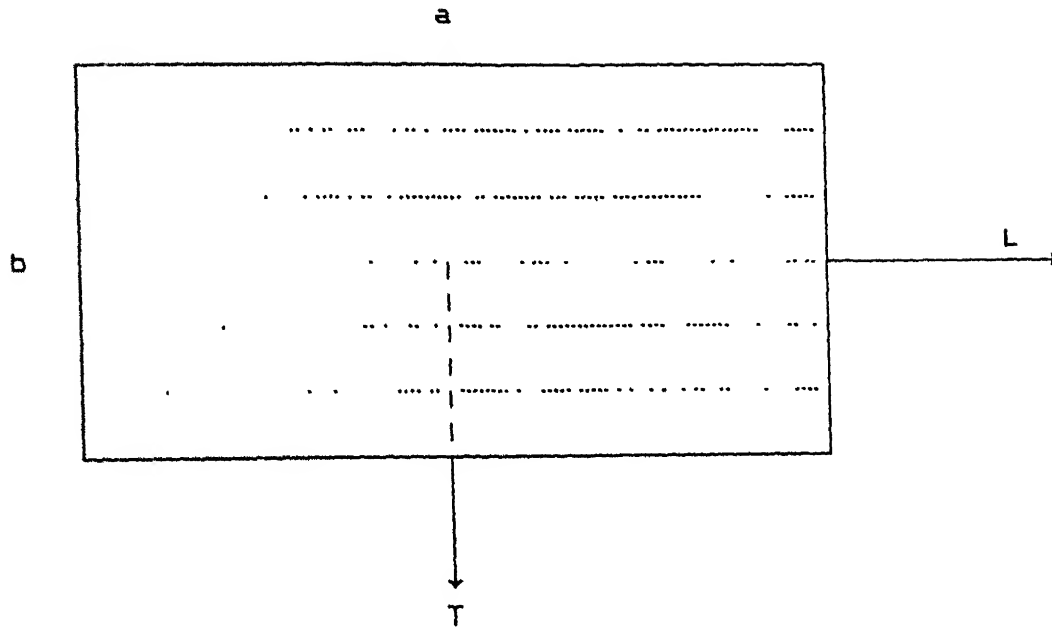


Fig. A1.1 Orthotropic lamina oriented along its principal coordinate axes.

The principal directions of orthotropy often do not coincide with coordinate directions that are geometrically natural to the solution of the problem (Fig. A1.2). Stress strain relationship for such lamina under plane stress are

$$\begin{Bmatrix} \sigma_x \\ \sigma_y \\ \tau_{xy} \end{Bmatrix} = \begin{bmatrix} \bar{Q}_{11} & \bar{Q}_{12} & \bar{Q}_{16} \\ \bar{Q}_{12} & \bar{Q}_{22} & \bar{Q}_{26} \\ \bar{Q}_{16} & \bar{Q}_{26} & \bar{Q}_{66} \end{bmatrix} \begin{Bmatrix} \epsilon_x \\ \epsilon_y \\ \gamma_{xy} \end{Bmatrix} \quad (\text{A1.3})$$

where the transformed reduced stiffness \bar{Q}_{ij} can be written in terms of reduced stiffness Q_{ij} in the following manner

$$\begin{aligned}
\bar{Q}_{11} &= Q_{11} C^4 + Q_{22} S^4 + 2(Q_{12} + 2Q_{66}) S^2 C^2 \\
\bar{Q}_{22} &= Q_{11} S^4 + Q_{22} C^4 + 2(Q_{12} + 2Q_{66}) S^2 C^2 \\
\bar{Q}_{12} &= (Q_{11} - Q_{22} - 4Q_{66}) S^2 C^2 + Q_{12} (C^4 + S^4) \\
\bar{Q}_{66} &= (Q_{11} + Q_{22} - 2Q_{12} - 2Q_{66}) S^2 C^2 + Q_{66} (S^4 + C^4) \\
\bar{Q}_{16} &= (Q_{11} - Q_{12} - 2Q_{66}) C^3 S - (Q_{22} - Q_{12} - 2Q_{66}) C S^3 \\
\bar{Q}_{26} &= (Q_{11} - Q_{12} - 2Q_{66}) C S^3 - (Q_{22} - Q_{12} - 2Q_{66}) C^3 S
\end{aligned}
\tag{A1.4}$$

where $C = \cos \theta$, $S = \sin \theta$ and θ is the angle from X-axis to principle orthotropic axis (L-axis) as shown in Fig.(A1.2)

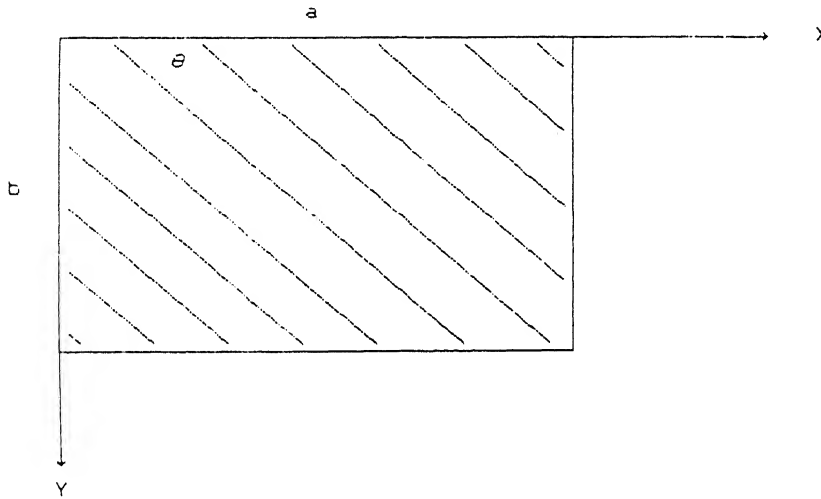


Fig. A1.2 Orthotropic lamina with its principal axes oriented at angle θ with reference coordinate axes.

Thus, in body coordinates, even an orthotropic lamina appears to be anisotropic. However, because such a lamina does have orthotropic characteristics in principal material directions, it is called generally orthotropic because it can be represented by stress-strain relations given by Eq.(A1.3). The Eq.(A1.3) can be thought of as stress-strain relations for the k^{th} layer of a multilayered laminate. Thus it can be written as

$$\begin{bmatrix} \sigma \end{bmatrix}_k = \begin{bmatrix} \bar{Q} \end{bmatrix}_k \begin{Bmatrix} \varepsilon \end{Bmatrix}_k \quad (\text{A1.5})$$

1.2 STRAIN VARIATION IN A LAMINATE :

The laminate is presumed to consist of perfectly bonded laminae. The bonds are infinitesimally small as well as non-shear-deformable; that is, the displacements are continuous across lamina boundary so that no lamina can slip relative to another. The Kirchhoff's hypothesis implies a linear variation of strain through the laminate thickness. The strain in the k^{th} layer can be expressed as

$$\begin{Bmatrix} \varepsilon_x \\ \varepsilon_y \\ \gamma_{xy} \end{Bmatrix}_k = \begin{Bmatrix} \varepsilon_x^0 \\ \varepsilon_y^0 \\ \gamma_{xy}^0 \end{Bmatrix} + z \begin{Bmatrix} K_x \\ K_y \\ K_{xy} \end{Bmatrix} \quad (\text{A1.6})$$

where the middle surface strains are

$$\begin{Bmatrix} \varepsilon_x^0 \\ \varepsilon_y^0 \\ \gamma_{xy}^0 \end{Bmatrix} = \begin{Bmatrix} \partial u_0 / \partial x + 1/2 (\partial w / \partial y)^2 \\ \partial v_0 / \partial y + 1/2 (\partial w / \partial x)^2 \\ \partial v_0 / \partial x + \partial u_0 / \partial y + (\partial w / \partial x)(\partial w / \partial y) \end{Bmatrix} \quad (\text{A1.7})$$

and the middle surface curvature can be expressed as

$$\begin{Bmatrix} K_x \\ K_y \\ K_{xy} \end{Bmatrix} = - \begin{Bmatrix} \partial^2 w / \partial x^2 \\ \partial^2 w / \partial y^2 \\ 2 \partial^2 w / \partial x \partial y \end{Bmatrix} \quad (\text{A1.8})$$

Here u_0 and v_0 are the middle surface displacements in the x - and

y-directions, respectively, and w is the lateral displacement.

1.3 RESULTANT FORCES AND MOMENTS OF A LAMINATE.

The resultant forces and moments acting on the cross-section of the laminate are defined as follows

$$(N_x, N_y, N_{xy}) = \int_{-H/2}^{H/2} (\sigma_x, \sigma_y, \tau_{xy}) dz \quad (A1.9)$$

$$(M_x, M_y, M_{xy}) = \int_{-H/2}^{H/2} (\sigma_x, \sigma_y, \tau_{xy}) z dz \quad (A1.10)$$

These force (N_x, N_y, N_{xy}) and moment (M_x, M_y, M_{xy}) resultants for a laminate can be related to the middle surface displacement components (u_0, v_0, w) , thermal forces (N_x^T, N_y^T, N_{xy}^T) and thermal moments (M_x^T, M_y^T, M_{xy}^T) by using expression (A1.11) and (A1.12)

$$\begin{Bmatrix} N_x \\ N_y \\ N_{xy} \end{Bmatrix} = \begin{bmatrix} A_{11} & A_{12} & A_{16} \\ A_{12} & A_{22} & A_{26} \\ A_{16} & A_{26} & A_{66} \end{bmatrix} \begin{Bmatrix} \epsilon_x^0 \\ \epsilon_y^0 \\ \gamma_{xy}^0 \end{Bmatrix} + \begin{bmatrix} B_{11} & B_{12} & B_{16} \\ B_{12} & B_{22} & B_{26} \\ B_{16} & B_{26} & B_{66} \end{bmatrix} \begin{Bmatrix} K_x \\ K_y \\ K_{xy} \end{Bmatrix} - \begin{Bmatrix} N_x^T \\ N_y^T \\ N_{xy}^T \end{Bmatrix} \quad (A1.11)$$

$$\begin{Bmatrix} M_x \\ M_y \\ M_{xy} \end{Bmatrix} = \begin{bmatrix} B_{11} & B_{12} & B_{16} \\ B_{12} & B_{22} & B_{26} \\ B_{16} & B_{26} & B_{66} \end{bmatrix} \begin{Bmatrix} \epsilon_x^0 \\ \epsilon_y^0 \\ \gamma_{xy}^0 \end{Bmatrix} + \begin{bmatrix} D_{11} & D_{12} & D_{16} \\ D_{12} & D_{22} & D_{26} \\ D_{16} & D_{26} & D_{66} \end{bmatrix} \begin{Bmatrix} K_x \\ K_y \\ K_{xy} \end{Bmatrix} - \begin{Bmatrix} M_x^T \\ M_y^T \\ M_{xy}^T \end{Bmatrix} \quad (A1.12)$$

Here A_{ij} , B_{ij} and D_{ij} are called the extensional, the coupling and the bending stiffnesses, respectively, and are defined in terms of $(\bar{Q}_{ij})_k$ for the individual layers $k = 1, 2, \dots, N$:

$$(A_{ij}, B_{ij}, D_{ij}) = \sum_{k=1}^N \int_{z_{k-1}}^{z_k} (1, z, z^2) (\bar{Q}_{ij})_k dz \quad (A1.13)$$

$$(i, j) = (1, 2, 6)$$

The limits z_k and z_{k-1} are shown in Fig. A1.3. The thermal forces and moments appearing in Eq.(A1.11) and Eq.(A1.12) are defined as

$$\begin{Bmatrix} N_x^T & N_x^T \\ N_y^T & M_y^T \\ N_{xy}^T & M_{xy}^T \end{Bmatrix} = \sum_{k=1}^N \int_{z_{k-1}}^{z_k} \begin{bmatrix} \bar{Q}_{11} & \bar{Q}_{12} & \bar{Q}_{16} \\ \bar{Q}_{12} & \bar{Q}_{22} & \bar{Q}_{26} \\ \bar{Q}_{16} & \bar{Q}_{26} & \bar{Q}_{66} \end{bmatrix} \begin{Bmatrix} \alpha_x \\ \alpha_y \\ 2\alpha_{xy} \end{Bmatrix} (1, z) T dz \quad (A1.14)$$

where α_x , α_y are the coefficients of thermal expansion in X- and Y-direction respectively, and α_{xy} is an apparent coefficient of thermal shear.

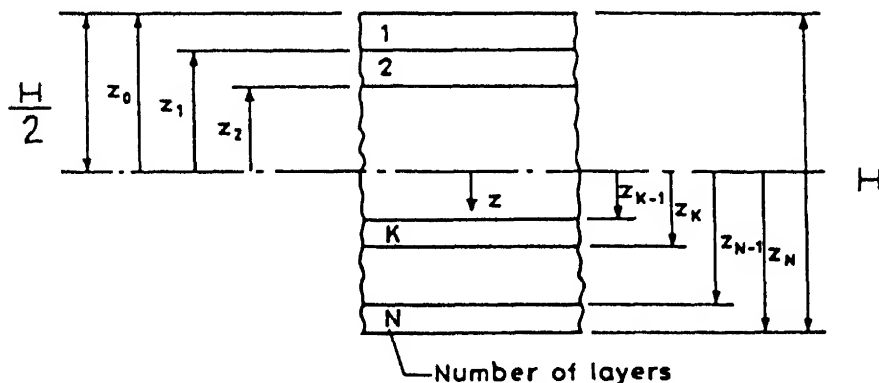


Fig.A1.3 Geometry of an N-layered laminate (Jones, 1975)

APPENDIX 2

1. Special cases of laminate stiffnesses

1.1 Antisymmetric Angle-ply Laminate

$$[A] = H \begin{bmatrix} \bar{Q}_{11} & \bar{Q}_{12} & 0 \\ & \bar{Q}_{22} & 0 \\ \text{sym.} & & \bar{Q}_{66} \end{bmatrix} \quad (\text{A2.1a})$$

$$[B] = \frac{-H^2}{2N} \begin{bmatrix} 0 & 0 & \bar{Q}_{16} \\ & 0 & \bar{Q}_{26} \\ \text{sym.} & & 0 \end{bmatrix} \quad (\text{A2.1b})$$

$$[D] = \frac{H^2}{12} [A] \quad (\text{A2.1c})$$

1.2 Symmetric Angle-ply Laminate

$$[A] = H \begin{bmatrix} \bar{Q}_{11} & \bar{Q}_{12} & \frac{1}{N} \bar{Q}_{16} \\ & \bar{Q}_{22} & \frac{1}{N} \bar{Q}_{26} \\ \text{sym.} & & \bar{Q}_{66} \end{bmatrix} \quad (\text{A2.2a})$$

$$[B] = 0 \quad (\text{A2.2b})$$

$$[D] = \frac{H^2}{12} [A] \quad (\text{A2.2c})$$

$$[A] = \begin{bmatrix} \frac{1}{2} Q_{11} (1 + \frac{1}{N}) + \frac{1}{2} Q_{22} (1 - \frac{1}{N}) & Q_{12} & 0 \\ Q_{12} & \frac{1}{2} Q_{11} (1 - \frac{1}{N}) + \frac{1}{2} Q_{22} (1 + \frac{1}{N}) & 0 \\ 0 & 0 & Q_{66} \end{bmatrix} \quad (A2.3a)$$

$$[B] = 0 \quad (A2.3b)$$

$$[D] = \frac{H^3}{12} \begin{bmatrix} \frac{1}{2} Q_{11} (1 + \frac{3}{N} - \frac{2}{N^2}) + \frac{1}{2} Q_{22} (1 - \frac{3}{N} + \frac{2}{N^2}) & Q_{12} & 0 \\ \text{sym} & \frac{1}{2} Q_{11} (1 - \frac{3}{N} + \frac{2}{N^2}) + \frac{1}{2} Q_{22} (1 + \frac{3}{N} - \frac{2}{N^2}) & 0 \\ & & Q_{66} \end{bmatrix} \quad (A2.3c)$$

1.5 Antisymmetric Cross-ply laminate

$$[A] = H \begin{bmatrix} \frac{Q_{11} + Q_{22}}{2} & Q_{12} & 0 \\ & \frac{Q_{11} + Q_{22}}{2} & 0 \\ \text{sym} & & Q_{66} \end{bmatrix} \quad (A2.4a)$$

$$[B] = -\frac{H^2}{4N} \begin{bmatrix} Q_{11} - Q_{22} & 0 & 0 \\ & Q_{22} - Q_{11} & 0 \\ \text{sym} & & 0 \end{bmatrix} \quad (A2.4b)$$

$$[D] = \frac{H^2}{12} [A] \quad (A2.4c)$$

It can be seen from Eqs. (A2.1)-(A2.4) that as the number of layers increases (i) the coupling stiffnesses tend to zero (ii) the extensional stiffnesses A_{16} and A_{26} , in the case of symmetric angle-ply laminate, tend to zero

Hence, the laminate behaves as a single specially orthotropic layer since B_{1j} , A_{16} , A_{26} , D_{16} and D_{26} are zero. Hence the solution corresponding to $N = \infty$ is termed as the orthotropic solution.